

Modeling the Effect of Spherical Particles of various sizes using Direct Laser Deposition



Zia Ur Rehman Sarwar

00000205599

Supervisor

Dr. Khalid Mahmood

Department of Mechanical Engineering

Collage of Electrical and Mechanical Engineering (CEME)

National University of Science and Technology (NUST)

Rawalpindi

September 2020

Modeling the effect of Spherical Particles of various sizes using Direct Laser Deposition

NS ZIA UR REHMAN

Registration # 00000205599

A thesis submitted in partial fulfillment of the requirements for the
degree of MS Mechanical

Supervisor

Dr. Khalid Mahmood

Supervisor's Signature:



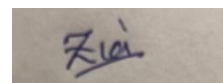
Department of Mechanical Engineering

**Collage of Electrical and Mechanical Engineering (CEME)
National University of Science and Technology (NUST)
Rawalpindi**

September 2020

DECLARATION

I certify that this research work titled “*Modeling the Effect of Spherical Particles of various Sizes using Direct Laser Deposition* ” is my own work. The work has not been presented elsewhere for assessment. The material that has been used from other sources has been properly acknowledged / referred.

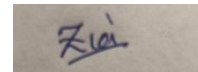


Signature of Student

NS Zia ur rehman Sarwar
00000205599

LANGUAGE CORRECTNESS CERTIFICATE

This thesis has been read by an English expert and is free of typing, syntax, semantic, grammatical and spelling mistakes. Thesis is also according to the format given by the university.



Signature of Student

NS Zia ur rehman sarwar

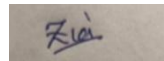
00000205599



Signature of Supervisor
(Dr Khalid Mahmood)

Plagiarism Certificate (Turnitin Report)

This thesis has been checked for Plagiarism. Turnitin report endorsed by Supervisor is attached.



Signature of Student

Zia Ur Rehman Sarwar

Registration Number

00000205599



Signature of Supervisor

COPYRIGHTS STATEMENT

- Copyright in text of this thesis rests with the student author. Copies (by any process) either in full, or of extracts, may be made only in accordance with instructions given by the author and lodged in the Library of NUST College of E&ME. Details may be obtained by the Librarian. This page must form part of any such copies made. Further copies (by any process) may not be made without the permission (in writing) of the author.
- The ownership of any intellectual property rights which may be described in this thesis is vested in NUST College of E&ME, subject to any prior agreement to the contrary, and may not be made available for use by third parties without the written permission of the College of E&ME, which will prescribe the terms and conditions of any such agreement.
- Further information on the conditions under which disclosures and exploitation may take place is available from the Library of NUST College of E&ME, Rawalpindi.

ACKNOWLEDGEMENTS

First of all I am grateful to **ALLAH**, who has given me guidance, strength and enabled me to accomplish this task. The journey on this road of success had not been possible without His will, and henceforth, all this success and accomplishment, I owe it to Him, in totality.

I want to thank my Parents for their support and prayers. They have been a driving force and without their support I might not have been able to get done with my thesis. I am grateful to my siblings, friends and well-wishers for their untiring support.

I would like to express gigantic gratitude to my supervisor **Dr Khalid Mahmood**, for his help and motivation throughout this journey of completing my research work. Without his help I would have not been able to accomplish this tedious job. Under his guidance, I am able to achieve my goals. He helped me throughout this journey of research and I'm really grateful for his unfailing support and assistance throughout my work.

I would like to thank my GEC member **Dr Nadeem Ahmad Shaikh** for his willingness to offer me his precious time and intellect during my research.

I would like to thank my GEC member **Dr Tariq Talha**, for broadening my concepts and guideline about research outline.

DEDICATION

I dedicate this work to my Parents and Siblings for their support, love and guidance. I appreciate their encouragement during all phases of my research and studies.

ABSTRACT

Additive manufacturing (AM) is the systematize name to describe the new world of manufacturing technology that built 3D objects by adding materials in layers, whether the material is in plastic, ceramics, metal and or it is advancing towards human tissues. Additive manufacturing (AM) technique of direct laser deposition (DLD) allows quick fabrication of fully-dense metallic components directly from Computer Aided Design (CAD) solid models. Direct Laser deposition (DLD) is ever-increasing in modern advanced manufacturing field for rapid manufacturing, tooling repair or surface enhancement of the critical metal components. DLD is based on a kind of directed energy deposition (DED) technology which ejects a strand of metal powders into a moving molten pool caused by energy-intensive laser to finally generate the solid tracks on the work piece surface. This method has a great possibility to reduce material waste through near net shape production as well as adding value to an already manufactured costly component (aviation and aerospace industry).The purpose of this study is to investigate the effect different size of spherical shape powder will have in direct energy deposition (DED).Powder size plays important role in determining the height, width of each track. Proposed modeling considerations and a specific CFD model of powder feeding will assist in accurately simulating the DED process. The results of these investigations have also been validated with an experimental work.

Table of Contents

DECLARATION	iii
LANGUAGE CORRECTNESS CERTIFICATE	iv
Plagiarism Certificate (Turnitin Report)	v
COPYRIGHTS STATEMENT	vi
ACKNOWLEDGEMENTS	vii
DEDICATION	viii
ABSTRACT	ix
List of Figures	xii
List of Tables	xiii
Chapter 1 INTRODUCTION	1
1.1. Background	1
1.2. Introduction:	2
1.3. Lagrangian-Eulerian Approach:	3
Chapter 2 LITERATURE REVIEW	4
2.1. Advance in Additive Manufacturing	4
2.2. Directed energy deposition (DED)	6
2.3. DLD	7
2.4. Laser:	8
2.5. Feed Materials:	9
2.6. Powder Feeding and Delivery:	9
Chapter 3 Modeling METHODS	19
Chapter 4 MODELING TECHNIQUE AND POST PROCESSING	25
4.1. Modeling Technique:	25
4.2. Post Processing:	34
4.3. Temperature Distribution:	36
Chapter 5 RESULTS and Discussions:	48

References.....49

List of Figures

Figure 2.1: Process categories, corresponding technologies and materials....	18
Figure2.1: Direct deposition.....	20
Figure2.3: Schematic of direct energy deposition.....	20
Figure 2.4: Coaxial nozzle, Multiple stream flow nozzle.....	22
Figure 2.5: Mesh of different sizes to measure particle size.....	22
Figure 2.6: Mesh of different sizes to measure particle size.....	25
Figure 2.7 Inter-Track (b) Interr-layer (c) Intra-layer.....	27
Figure 3.1: Schematic of two particles in contact.....	34
Figure 4.1: Mfix parameters.....	37
Figure4.2: Meshing of Nozzle and Geometry.....	43
Figure 4.3: Volume fraction of solid particles.....	48
Figure 4.4: Particles Motion through nozzle into bed.....	49
Figure 4.5: Temperature Distribution at 0.05s.....	49
Figure 4.6.: Temperature Distribution at 0.1s, 0.2, 0.3 and 0.4s.....	50
Figure 4.7: Temperature distribution at 0, 0.1,0.2s.....	51
Figure 4.8: Temperature distribution at 0.28,0.333,0.4s.....	54
Figure 4.9: Particle Drop through nozzle.....	55
Figure 4.10: Layer Formation.....	56
Figure 4.11: Layer Formation.....	56
Figure4.12: Layer Formation.....	57
Figure 4.13: Mass flow rate vs layer build height of small particles.....	58
Figure 4.14: Mass flow rate vs layer build height of large particles at 800W....	58
Figure 4.15: Mass flow rate vs layer build height of small particles at 1000W.....	59
Figure4.16: Mass flow rate vs layer build height of large particles at 1000W.....	59

List of Tables

Table 2.2: Process categories, corresponding technologies and materials.....	16
Table 3.1. Particle Size Distribution.....	36
Table 4.1: Factors showing variation in this whole process.....	40
Table 4.2. Numerous variable Process parameters.....	41
Table 4.3: Simulation Parameters.....	41
Table 4.4: x-y-z Length.....	42

CHAPTER 1 INTRODUCTION

1.1. Background

Directed energy deposition (DED) process, in additive manufacturing frame is gaining more interest in industry due to its more effectiveness and minimum invasiveness [1,2]. This technology involves the surface scanning through laser beam to create melting pool on existing substrate and later metal is fed either in form of powder or wire in a process of a single stage. Hence, additional metal can also be applied on the worn-out surfaces to restore the nominal dimensions as well as prevent the part disposal. With this objective, researchers investigated the technology over the flat surfaces [3], damaged edges by using technology in challenging deposition conditions [4]. Further, this process has also been considered for freeform fabrication purpose, with aim of controlling metal crystal orientation and to control residual pores in super alloys [5]. Hence, it is argued that DED have high potential in large scale automotive production as well as aerospace [6].

Source, material and focused energy are fed simultaneously in desired regions during the DED process. Feeding material along with pre-deposited layers is melted simultaneously to create liquid material named as melt-pool. Melted material again solidifies and connects with pre-deposited material in form of a bond and builds new layers in a short time span. DED process often uses the laser [7] and electron beam [8, 9] as energy source. Further, DED machines may also use feeding material like wire [11], powder [10] or even both. Further, Syed et al. [12] also compared the feeding methods and Syed et al. [13], examined the feeding methods by examining their potential combination. DED process using laser powder is named as direct laser deposition (DLD) [14], and powder is injected on focused region with coaxial or multi-jet nozzle and help of carrier as well as shielding gas in order to increase deposition efficiency and decrease potential oxidation. While, in some features, the wire-based DED may outperform the DLD like in efficiency of process and quality of surface. Though, power delivery may efficiently be achieved through wire feeding machine while accurate fabrication may be achieved with powder based machines. In addition to this, DLD offers more convenience and diversity by enabling the parts fabrication with complex geometries and more customized features. In order to shape

graded part, DLD may utilize different powder sources (e.g., [15–17]). DLD is also used for repairing purposes (e.g., [18–20]) as well as cladding operations (e.g., [21, 22]). DLD concept was came up decades ago like process of laser engineered net shaping (LENS) [23].

1.2. Introduction:

A gas–solids flow comprises of chemical, food, agriculture processing, energy production and pharmaceutical and involve in various industrial processes. They are also involved in natural phenomena's like cosmic dusts as well as sand storms. Accurate and proper understanding of gas solid flow is needed in order to improve design as well as operations of industrial processes and insure accuracy in natural phenomena's, which involves gas solid flow. Computational algorithms CFD modeling is employed to achieve goals due to high speed computers.

Eulerian–Eulerian (EE) approach, or the two-fluid model (TFM) and Lagrangian–Eulerian (LE) approach are the main methods employed for simulating gas–solids flows. In approach of Eulerian–Eulerian, every phase is considered as interpenetrating continuum. Further, conservation equations of momentum, energy and mass for particulate and fluid both are derived through averaging technique [24,25]. This process offers unknown terms which need conclusion models like drag force and stresses). kinetic theory is employed to derive the constitutive relations specifically for solids phase[26,27]. Nevertheless, for this determination, many relations have been proposed [28,29]. In approach of Lagrangian–Eulerian (LE), Newton's motion laws involving collisions of particles and forces are resolved for every particle. Further, other approaches of CFD modeling like discrete bubble model, direct numerical simulation (DNS) and lattice-Boltzmann method may be found in previous studies [30]). Both approaches has few advantages and disadvantages as well. For instance, LE approach is comparatively straightforward to model particles with different sizes and densities in contrast to EE method .

In flow of fluid–particle, interphase momentum conversation has significant role to vary features of particle transport as well as sedimentation [31–32]. Term computed depends on multiphase illustration which is chosen and it can be either Eulerian–Eulerian) or Eulerian–Lagrangian (EL).

1.3. Lagrangian-Eulerian Approach:

Approach of Lagrangian Eulerian (LE) calculates multiphase flows properties like sprays and particle-laden flows which are usually encountered in various energy applications. LE method denotes modeling family and also simulation techniques with droplets represented as Lagrangian reference frame and carrier-phase flow field as the Eulerian frame.

If LE approach is used as predictive tool in simulation methodology, it should include:

- Mathematical representation to show physical phenomena
- Consistent and correct models specifically for unclosed terms
- Numerically stable as well as convergent implementation.

Challenges in these areas should be overcome to develop LE simulation approach for purpose of multiphase flows. LE approach has benefit over EE approach because LE has more capacity to measure the collision in flow. Accordingly, it is observed that connection due to flow may modify attributes of collisions in particle-laden as well as droplet-laden flow. Effective restitution coefficient is particle function [33]. Such effects can be assimilated in LE approach easily. Further, LE method decreases numerical diffusion in volume fraction as well as mean velocity in contrast to approaches of grid-based Eulerian.

CHAPTER 2 LITERATURE REVIEW

2.1. Advance in Additive Manufacturing

AM encompassing many specific technologies is considered a very comprehensive process. These technologies are further categorized into seven types based on different techniques employed for layers deposition and the way layers are bonded further to make a track [34]. These seven categories as per recommendations of ASTM F42 committees are given below:

1. Material jetting (e.g., multi-jets modeling abbreviated as MJM)
2. Material extrusion (e.g. fused deposition modeling abbreviated as FDM)
3. Sheet lamination (e.g. laminated object manufacturing abbreviated as LOM)
4. Vat photo polymerization (e.g. Stereolithography abbreviated as SLA)
5. Binder jetting (e.g. 3D printing abbreviated as 3DP)
6. Powder bed fusion (e.g., SLM, EBM, SLS)
7. Directed energy deposition (e.g. DLD/LENS, EBAM).

Table 2.3: Process categories, corresponding technologies and materials for existing AM processes

Process category	Specific technology	Corresponding Materials
Vat photo polymerization	Stereolithography (SLA)	UV curable resins
Material jetting	MJM (multijet modeling)	waxes, ceramics, UV curable resins
Binder jetting	3DP (3D printing)	waxes, composites, polymer, ceramics, metals, thermoplastics
Powder bed fusion	SLS, SLM, EBM(electron beam melting)	waxes, thermoplastics, metals metals metals
Sheet Lamination	LOM	Paper, metals, thermoplastics

Directed energy deposition	Directed energy deposition	Metals
----------------------------	----------------------------	--------

Table 2.1 describes the category names as well as corresponding materials and also corresponding technologies which are to be used for seven categories of these AM processes. AM process may also be divided into 4 categories based on materials used. For example, on the basis of liquid, solid sheet, filament/paste and powder used in AM process [35]. Hence, after recent research and development in areas like processes, equipment, integration, materials and software, it can be argued that AM with suitable material is employed directly as well as indirectly for producing prototype parts to evaluate and test and also for develop dies, molds and tools. Recently, direct fabrication of end-use products has become the main trend through usage of AM technologies and particularly for the metallic products [36].

AM process if used offers easy access to create the manufactured parts, instead of using casting or milling and die cutter which otherwise is needed. Further, a lot of material is usually wasted during the process of cutting. While, this wastage can be avoided with the usage of net shape production through AM technology because it employs the material required for finished product. AM technology also requires support material in shape of structures during some specific production cases. However, these requirements still do not outweigh the wastes which may arise from employing other production methods.

Casting depends on pre-existing mould, making this process inappropriate because it may narrow down the manufacturing market especially for certain products for some companies and for global location as well. It may also be applied to pressing process by using pre-existing die cutter and also wasting the additional material from finished product. Further, one deficiency of casting technology is dearth of possibility of production for the hollow parts. Hence, AM process is considered highly appropriate and advanced to accomplish this goal.

Different materials may also be employed in manufacturing process of additive like food products, glass, plastic and metals. This study focuses on metal AM because this research concentrated on metal with two different particle sizes. AM process involving metal has three subcategories as mentioned below:

1. Deposition technologies
2. Powder-bed technologies

3. Laminated object manufacturing

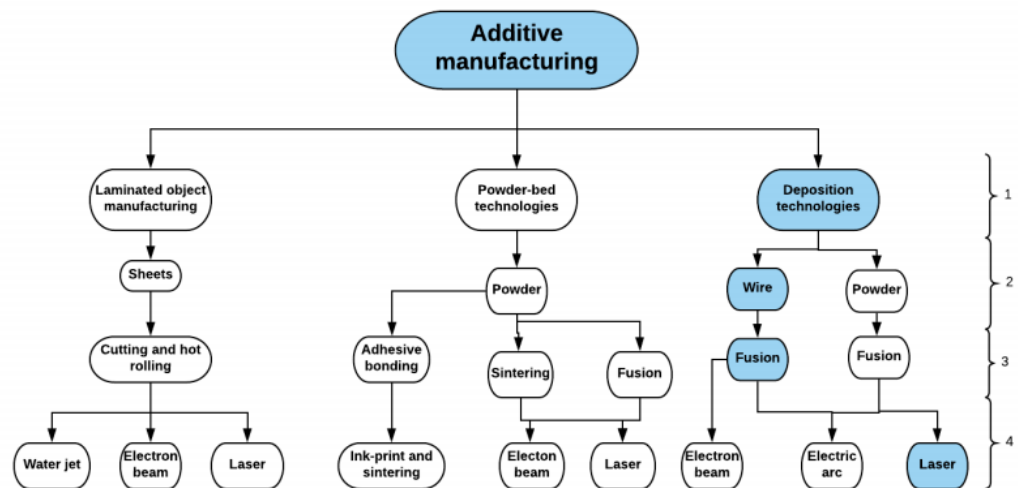


Figure 2.2: Flowchart overview of the AM process.

Arrows mark the different technologies which may be used by AM processes and highlighted fields demonstrate the LMWD technology. First sublevel reveals the AM method, second explains the bonding method for different materials and third level illustrates the available energy sources [37]. Further, energy sources used employed by AM process may vary. However, most common are electron beams, laser beams and electric arcs. DLD (DLD) is subcategory is found in category of direct energy deposition (DED). In this process, a wire or some powder is usually fed in melt pool which is generated on substrate surface, where melted wire adheres with underlying substrate. Wire is heated through some energy source like laser or the electron beam and it is considered form of automated build-up welding [38]. Main focus of this research is Laser metal wire deposition (LMWD)

2.2. Directed energy deposition (DED)

Directed energy deposition (DED) which is one category out of 7 categories of AM process is appropriate to produce metal parts through layer-by-layer deposition of melted metal filament and melted metal powder. It also uses laser or the electron beam as energy source to create the metal pool on substrate where the injection of metal powder or filament is induced. Further, molten pool then moves on a specific route to fill the substrate top and builds as well as deposits the part following the CAD geometry. This standard category may employ various AM technologies like “laser-

engineering net shaping (LENS), Direct Laser Deposition (DLD), laser deposition welding and powder fusion welding, DLD (DLD), direct metal deposition (DMD) and laser consolidation, laser cladding” and out of these various are trademarks of many research establishments and machine manufacturers. Further, it is important to note that local high-energy in the process of DED may effect the residual stress state, deposited material properties, thermal-induced distortion and microstructure.

2.3. DLD

DLD is from AM category of the process DED. DLD employs a laser beam to generate a molten pool on substrate and then powder is fed into this substrate. Powder is melted then and deposited track is developed on substrate through bonded fusion. This type of laser of AM process is found to have a material and process dependent non-equilibrium physical as well as chemical metallurgical nature. Currently, DED/DLD is used to generate many complex shaped metallic components which involves alloys, metal matrix composites (MMCs) and metals in order to meet requirements and demands of defense, biomedical industries, aerospace and automotive. Effect of characteristics of material and conditions of processing on the metallurgical mechanisms and resulting mechanical as well as microstructural properties of components after DLD process are needed to be explained.

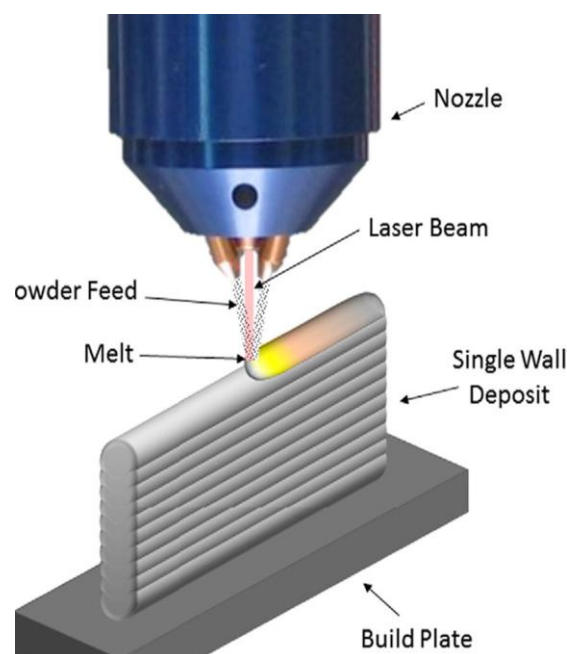


Figure 2.3: Direct laser deposition.

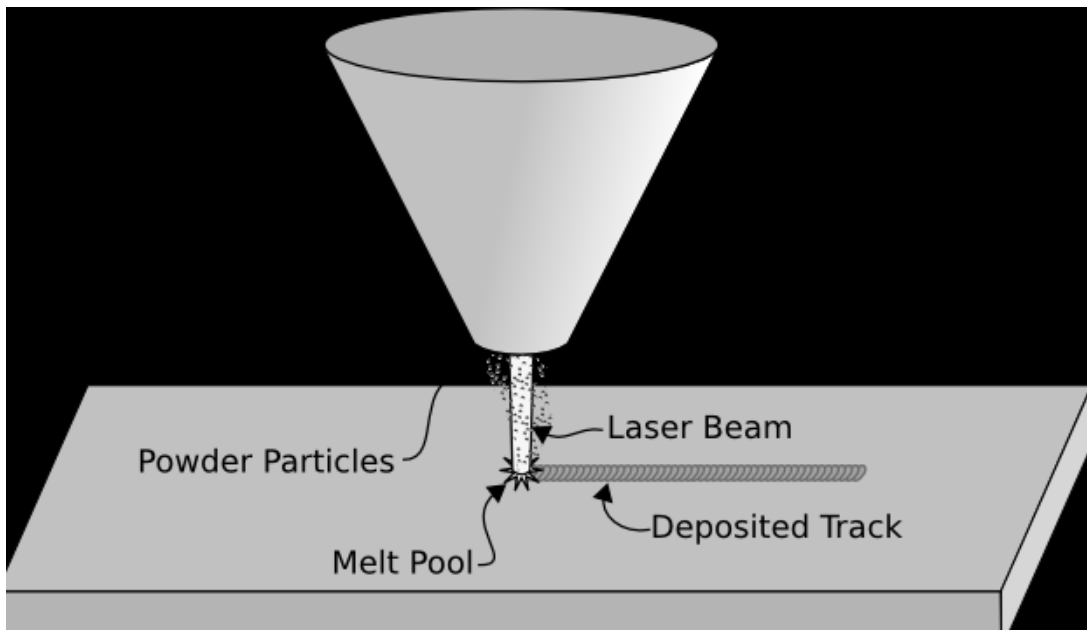


Figure 2.3: Schematic of direct energy deposition

Process involves following subsystems

- Laser (as heating source)
- System of material delivery
- Mechanism of traversing and shielding

2.4. Laser:

Laser is considered as most amazing finding of previous century with numerous applications in era of modern manufacturing. Laser process refers to monochromatic, lucid electromagnetic radiations and optical amplification with higher intensity characteristics. Laser word is acronym of “Light Amplification by Simulated Emission of Radiation” . Laser is used for heating powder to make it melt in normal and controlled way so that it could solidify again speedily. DLD processes use lasers commonly named YAG laser, fiber laser, carbon dioxide (CO₂) laser and diode laser.

In this research, two laser power is used to investigate its impact on mechanical properties by using two different sizes of powder which would help to develop a relation.

2.5. Feed Materials:

This process usually employs metals which can be either powder or wire mostly, but DED may also use polymers and ceramics also. For instance, for applications of end use, AREVO employs Polymer DED with carbon fiber filament for fabrication of lightweight composite parts. Further, heat source melts the thermoplastic filament and roller compacts it to create layers. Any metal which is weldable may be 3D printed through DED. For example, aluminium, inconel, tungsten, stainless steel, titanium, tantalum and niobium etc. wire used had diameter range from 1-3 mm and powder particle sizes are same as used in processes of powder metallurgy that is 50 and 250 micron. This study uses different stainless steel 316L spherical powder particles.

2.6. Powder Feeding and Delivery:

Powder form is considered as proficient feedstock material because mostly ceramic materials as well as metals are available in form of powder. Further, many types of powder feeders are available as per working feasibility. For example, these may be feeder of gravity-fed powder [40], feeder of vibratory powder [41] and hoppers [39]. During the whole process, all powder is not covered in melt pool. Hence, in order to have the excessive powder amount a system should be there to recapture it in a uncontaminated form. In process of DLD, in order to make melt pool look like as shown is figure 4.

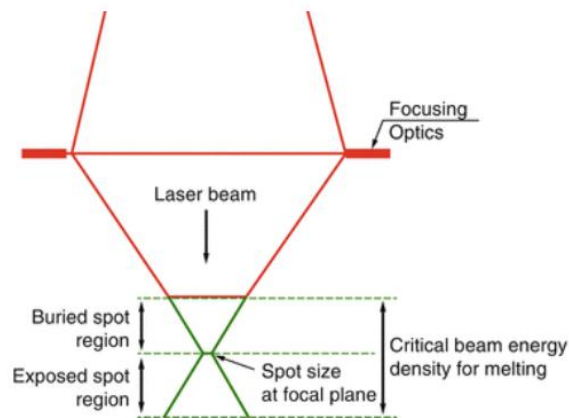


Figure 2.4: DLD parameters.

Main thing is energy density in laser beam which should be above than a critical amount. Nozzle is used to deliver the powder, hence according to process complexity different shapes of nozzles may be used.

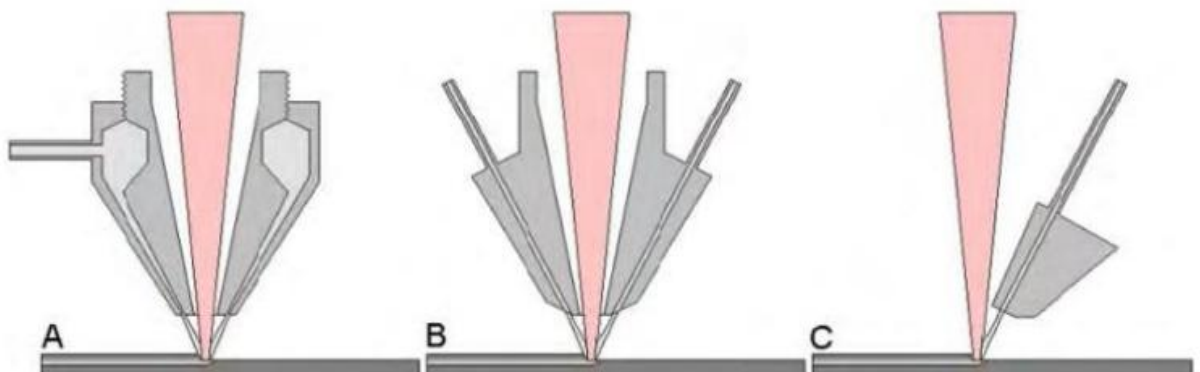


Figure 2.5 : Coaxial nozzle (B)Multiple stream flow nozzle (C) Single feeding Nozzle

a) Coaxial Nozzle: In this type of nozzle, powder surrounding the laser beam is fed with focus on narrow point while using inert gas shielding in order to avoid contamination.

b) Multi Axis Nozzle:

It introduces the powder stream to laser source via multi axis. Here the single lateral nozzle is converged between beam of laser and substrate focusing on intersecting point. This type of nozzle has multiple nozzle heads with equal space and all heads are concentrated towards melt pool. The lateral nozzle when reaches complex points, it has circular outlet [42].

c) Shielding and Traversing:

In DLD process, inert gasses provide shielding to minimize oxidation. Researchers have used Argon [44], Nitrogen [45] and Helium [43] for this purpose.

d) Processing Features for DLD

i. Build Material

DLD processes have an aim to generate 3D end products. Stable powder material in molten pool may be used for parts of production. Material is used in form of powder as well as wire but powder is usually preferred form. It has benefit of regulating the clad dimension. Generally, in DLD process metals like aluminum alloys or gold having high thermal reflectivities as well as thermal conductivities are not easy to process. Metallic materials with good weldability quality can be processed reasonably. Powder refers to processed from of ceramics as well as metals. grinding. Further, DLD also employs Gas atomized (GA) metal powder to produce powder particles of spherical shape [46].

Water atomized is considered cheap way to produce powder particles but these particles may take shape other than spherical shape [47].

ii. Processing Parameters

Variables in shape of processing parameters may effect the overall quality of process of laser deposition. Desired results are attained through careful selection. Important processing parameters are given below:

- Beam diameter
- Laser power
- Flow rate of powder mass
- Scanning speed

iii. Flow Rate of Powder Mass: It refers to quantity of material which is delivered in per unit time.

It effects dimensional accuracy of deposited layer and also final products mechanical properties [48].

iv. **Laser Power:** Deposited material is melted through energy source that is laser power and therefore effects the melt pool and its dynamics. DLD process may employ many types of lasers. Laser power differs from each other due to difference in wavelength and with increased wavelength metals absorption of laser is decreased [49].

v. **Beam Diameter:** Beam diameter decides laser's spot diameter which further determines the deposited layer width [50].

vi. **Scanning Speed:** Scanning speed refers to laser speed with which it traverses and in case if it is stationary then it moves with speed of substrate. It effects the quantity of deposited material as well as solidification time [51]. Other processing parameters which are also accounted for DLD process are mentioned as:

- Nozzle Geometry
- Feed Rate of Powder
- Residual Stress
- Injection Angle
- Carrier Gas Flow Rate
- Microstructure

e) **Effect of processing parameters:**

i. **Powder Size and Morphology**

Powder particles have following main features.

- Shape of particles and structure
- Size of particles

Particle size comprises powder particles dimensions. Different methods may be used for measuring the particle size. Most commonly used method is usage of screen of mesh sizes [52] , depicted in FIG 2. Sieving method is considered as one of the conventional method for measuring the particle size. Size of the particles id determined on the basis of mesh size.

MEASUREMENT OF POWDER PARTICLES

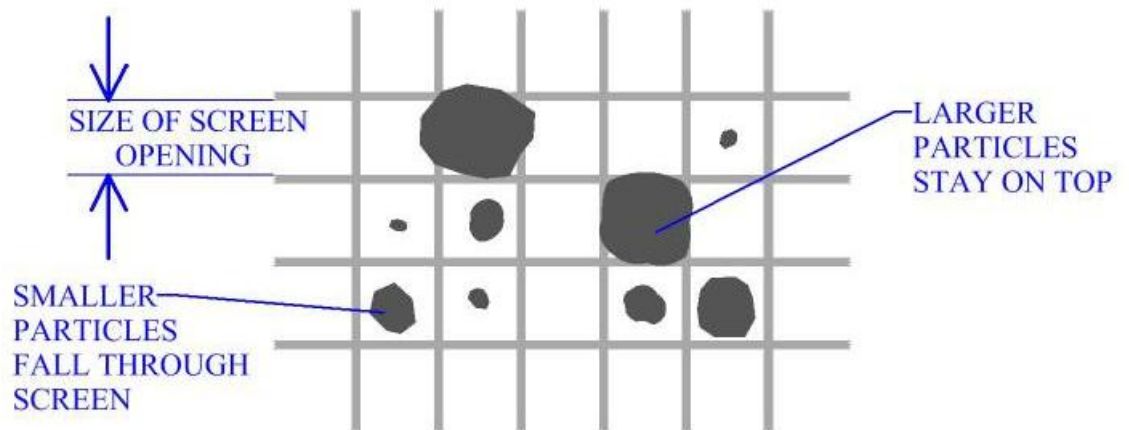


Figure 2.6: Mesh of different sizes to measure particle size

Particle size is measured from the formula given below

$$\text{Particle Size} = PS = 1/MC - tw$$

While, MC depicts mesh count, tw depicts wire thickness. Further, particles size may also be measured by employing other methods like laser x-ray diffraction [54] as well as microscopy [53]. Particles dimensions are categorized into types as:

- Spherical
- Non-spherical

Diameter is considered an important factor for calculation of spherical particle. size is measured approximately by employing aspect ratio. Further, it was concluded that particle shapes have three main categories named as :

- Spherical
- Near-spherical
- non-spherical

These are further sub categorized into following types as :

- Regular satellite
- elongated and irregular

- Particle dispersion is induced when deviation from spheres takes place, which greatly effects the focus of powder stream at exit of nozzle [55]. Size and shape of powder particles plays their huge role in process of DLD regarding their deposition quality as well as deposition efficiency. It is found that if shape of particles changes, it effects the deposited layer quality also. Accordingly, with increased size of particle size, decrease in laser power and laser energy is observed [56]. Changed size and shape may effect the particles the temperature distribution and ultimately have an impact on dynamics of melt pool [57].

DED process stages:

This process has further sub processes as:

- Final Track Microstructure
- Powder Stream Processes
- Melt Pool Processes

Melt pool:

Melt pool of AM process is same as is the weld pool generated in fusion welding process. In process of welding, heat source like laser beam, electron beam and electric arc may be used. Weld pool is effected by overpowering forces as discussed below:

Surface tension gradient:

Surface tension refers to shrinking tendency of fluid surfaces in the minimum possible surface. Surface tension depends on temperature and declines for high heat. Hence, edges of liquid show more surface tension because temperature is lowest around edges. Surface tension is the result of cohesion when liquid molecules attract each other while adhesion is attraction of molecules from air.

Electromagnetic forces:

It is named as Lorentz force which is produced by charged particles, q which moves with velocity denoted with \mathbf{v} , in electric field denoted with \mathbf{E} , as well as magnetic field denoted with \mathbf{B} . Formula is given as Equation , which measures the

Lorentz Force, \mathbf{F} in Tesla $[T]$, while velocity, \mathbf{v} in $[m=s]$, while particles charge is measured in coulomb $[C]$, electromagnetic field,

\mathbf{E} is measured in Volts per meter $[V=m]$ or $[N=C]$. Similarly, magnetic field, \mathbf{B} is measured in SI unit Gauss $[G]$ and is defined as $[force=charge]$ and Tesla is equal to $[Ns=Cm]$.

$$\mathbf{F} = q\mathbf{E} + q\mathbf{v} \times \mathbf{B} \quad (1.1)$$

Buoyancy:

Archimedes principle results in buoyancy force. it is an upward force which fluid exerts in opposition of immersed object weight. Fluid exerts more pressure at fluid bottom in fluid column as compared to upper areas. The difference in pressure creates upward force and named as buoyancy force.

Porosity

Pore and void formation is divided further into categories in process of DLD and named as:

- Inter-layer
- Intra-layer porosities
- Inter-track

These flaws are shown in figure below

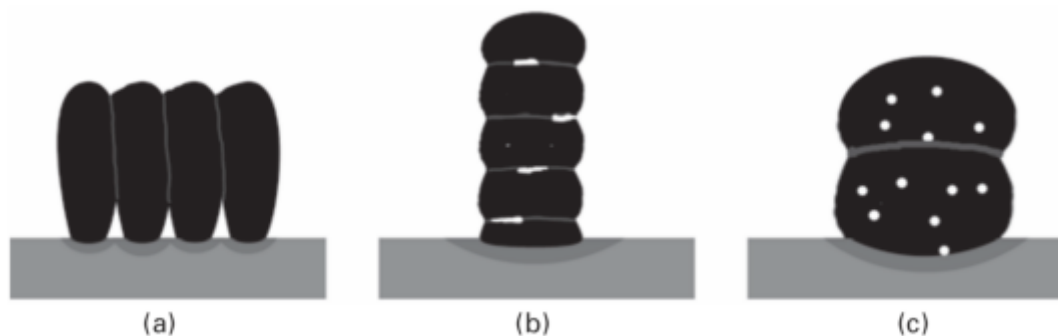


Figure 2.7 Inter-Track (b) Interr-layer (c) Intra-layer

Inter-track:

Inter track voids created by offset tracks or also by horizontally aligned aspect ratios. Deposited molten base does not adhere to substrate of deposited material and hence bubbles are generated near base.

Inter-layer:

Inter layer flaws are generated due to less fusion of vertically aligned deposition. There are many factors which may be the reason of this lack of proper fusion and include inconsistent energy, misplaced tracks and oxide layers.

Intra-layer:

Intra-layer porosity occurs in spherical areas in a layer. It is described in laser metal powder deposition via trapped gas among the powder particles. While, laser welding also found that voids may also be generated through moisture which exists in industrial-grade shroud gases. When power is increased, material vaporization may occur as problem.

Particle-fluid interactions

Four techniques are used in simulations of flow of particle. Techniques chosen depend on degree of dispersity specifically in multiphase flow. More bubble fluid is necessity for interaction of particle-particle in solver. It is not important for the dilute concentrations and only proceeds with the processing time. Four techniques are briefly described below:

One-way coupling:

Flow effects the particles movement. Particles show movement with same velocity in fluid and at the same time fluid is not affected by these particles. Particles get effected by buoyancy in this model, and buoyancy may cause particles to float or sink due to their mass.

Two-way coupling:

In this model, flow effects the particle movement and flow is also effected by particles existence. This means that fluid flow may get changed due to particle disturbances. Further, buoyancy effects may also cause feedback due to turbulence damping.

Four-way coupling:

It is almost same as is two-way coupling with only difference that here additional interaction is observed between particles as fluid streamlines are usually compressed between different particles and also particle-particle interaction. Hence, it may increase the possibility of collision and presence of friction.

Post-processing:

In this type, particles are added in period of post-processing to make the flow streamlined, providing no influence of particles over flow of fluid. Streamline if changed between the time steps may effect the trajectory of flow of particles.

Model outline

Model outline includes following:

- Deformation
- Evaporation
- Radiation
- Phase transitions
- Plasma
- Laser
- Geometry
- Pores.

Brief description of these given as:

Deformation:

It refers to possibility of melt pool to get deformed if laser beam is transverse.

Evaporation and addition of material:

It involves material loss through vaporization at surface of melt pool, or addition of melted alloy droplets from metal wire.

Radiation:

Heat may cause loss of energy through surface area.

Phase transitions:

Change of phases like vapors, liquid and solid need to be modeled. Also the change of metal alloy via mushy region should be observed and modeled.

Plasma:

Plasma put electromagnetic forces, pressure, Lorentz forces and energy on metal alloys.

Laser: It refers to heat source with Gaussian distribution, which traverse over substrate.

Geometry:

Geometry resembles process to best possible. Hence it is a melt track as leading end and semi melted tail which follows it.

Pores:

Pores must have 2-way-coupling referring that fluid effect the pores with possibility of pores interaction with each other. Pores may be of different shapes as well as different sizes.

Limitations:

Although, additive manufacturing process entails various positive factors, It also acknowledge few limitations mentioned below:

Pores:

Pores added during the post-processing. Hence, particles did not have an impact on flow as they showed lack of mass it was just a visualization of path generated for point source.

Laser:

Laser beam showed no reflection because laser applied during AM showed reflection from surface and pool.

Deformation:

Melt pool deformation especially at bottom and edges wasn't applied in mapping case and therefore, only surface edge was deformed. Lorentz force was not implemented also in model.

Phase transitions:

Change in one phase was considered only like solid melting to the fluid with no possibility of evaporation. Further, cooling and solidification was ignored too.

CHAPTER 3 MODELING METHODS

3.1. Modeling technique:

Gas and solid flows are used in many industrial processes as well as in numerous natural cosmic dusts and the sand storms. Two commonly used approaches employed for stimulating gas solid flows have been mentioned below:

- Eulerian Eulerian Method, abbreviated as EE
- Lagrangian Eulerian Method, abbreviated as LE

In approach of Eulerian-Eulerian(EE), every phase is considered as the interpenetrating continuum and further, mass, energy and momentum's conservation equations are employed for particle as well as fluid phase both. This process is used to find out the unidentified terms that are included in the closure models (e.g., stress and drag). Further, in approach of Lagrangian-Eulerian (LE), Newton's laws of motion which accounts to count the forces which may arise in process of particles collapse and forces which may act on particles in gas phase are resolved for every particle involved (Li, Garg, Galvin, & Pannala, 2012).

These methods involves few advantages as well as disadvantages as LE method is much simpler in contrast to EE method inorder to model solids with particles having different properties like size and density etc

3.2. Modeling Details:

This study employs LE method which involves Discrete Element Method (DEM). DEM is being employed since over the previous 30 years. This is numerical technique being employed for calculations of small particles interactions in large quantity (Manne). This approach estimates different types of particles displacements and rotation during flow simulations of particles. Cohesive forces (e.g., Van der Waals) may not play an important role in packing of particles together, if this approach is employed on microparticles (R. Tayeb). Further, particles size distribution is an important factor in powder system to determine about particles packing.

3.3. Computational Fluid Dynamics (CFD)

Computational fluid dynamics is considered a large subfield in the fluid dynamics. It's the area to provide numerical solutions specifically of fluid glitches. Problems involved here cannot be solved with just analytical approach, therefore, numerical solution is considered a good option. Domain which is to be estimated is named as control volume (CV). Further it expands over the body while covering surroundings also. Control mass and volume differ from each other as system does follow matter in case of control mass because mass flows, while volume remains same in case of control volume. Volume is further divided into distinct parts for purpose of computation which is named as discretization and are required for method of finite volume.

3.4. Discrete Element Method (DEM)

This method employs particles denoted by N_m with density ρ_{sm} , and diameter D_m show the microparticles flow. Further, particles total number is achieved by every spherical particle over the solid phases number denoted by M and is given below:

$$N = \sum_{m=1}^M N_m$$

Here, N particle may be defined via velocity, density, diameter, position, mass and angular velocity. Linear as well as angular velocities are attained using newton law as given:

$$\frac{dX^{(i)}(t)}{dt} = V^{(i)}(t)$$

$$m^{(i)} \frac{dV^{(i)}}{dt} = F_T^{(i)} = m^{(i)}g + F_a^{(i)}(t) + F_c^{(i)}(t)$$

$$I^{(i)} \frac{d\omega^{(i)}(t)}{dt} = T^{(i)}$$

While, X shows particle position at t , $\omega^{(i)}$ indicates angular velocity, V indicates linear velocity at time of i th particle and F_d shows the drag force, is achieved through summation of viscous forces as well as pressures. F_c indicates force which usually acts on particles when particles show contact.

3.5. Contact Forces

This analysis uses the spring dashpot mode to have interaction of particles and with base of particles of soft sphere model. This model also calculates the degree of overlapping in particles of two micro scale because it does not have any restriction for the contacts of multiple particles. Equation 5 is used to obtain overlap among particles, while unit vector with contact line between every particle is shown in equation 6.

$$\delta_n = 0.5 (D^{(i)} + D^{(j)}) - |X^{(i)} + X^{(j)}| \quad (5)$$

$$\eta_{ij} = \frac{(D^{(i)} + D^{(j)})}{|X^{(i)} + X^{(j)}|} \quad (6)$$

Where, in equation 5 for the soft sphere collision shown in figure below, two particles i and j of diameter $D^{(i)}$ and $D^{(j)}$ and are located at position $X^{(i)}$ and $X^{(j)}$ moves with linear velocity V and angular velocity ω .

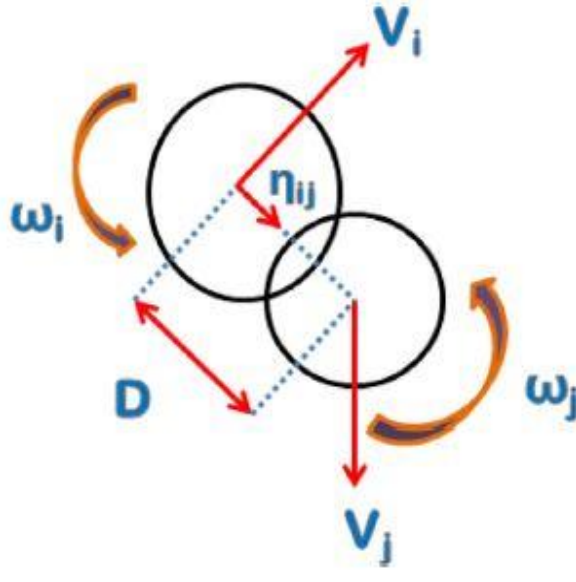


Figure 3.1: Schematic of two particles in contact

Heat conduction through particle contact is combined with heat generated with laser and is used as heat distribution. Hence, through power Q laser is set.

$$Q = kA\Delta T$$

K describes the coefficient of heat transfer. Laser power Q is determined by using above mentioned equation.

$$V_{ij} = V^{(i)} - V^{(j)} + (L^{(i)}\omega^{(i)} + L^{(j)}\omega^{(j)}) \times \eta_{ij}$$

While L describes the contact points distance from particles center i and j .

System of spring and dashpots presents the overlap between adjacent particles for soft sphere model in this study. In system of spring and dashpot, springs show elastic interaction among particles, however, dashpots indicate loss of kinetic energy due to inelastic collision. Springs stiffness is mentioned in tangential as well as normal directions. Stiffness depends on particles elastic module at interaction time. Likewise, each particle is given with dashpot damping coefficient and is determined through particles collision and their inelastic scattering. Relationship in normal dashpot coefficient and the normal coefficient of the restitution is :

$$\eta_{nml} = \frac{2\sqrt{m_{eff}k_{nml}|lne_{nml}|}}{\sqrt{\pi^2 + lne_{nml}^2}}$$

While, normal dashpot coefficient is η_{nml} and gives link with coefficient of the restitution. While, normal damping coefficient is as twice as tangential damping coefficient. Therefore, M x M symmetric matrices denotes this link and given below:

Coefficient of normal restitution matrix and tangential coefficient of restitution

$$[e_n] = \begin{bmatrix} e_{n11} & e_{n12} \cdots & e_{n1M} \\ \vdots & \ddots & \vdots \\ e_{nM1} & e_{nM2} \cdots & e_{nMM} \end{bmatrix}$$

3.6. Cohesive Forces:

Derjaguin Muller Toporov (DMT) model is used to model interaction of cohesive forces between particles as well as walls. Values of inner and the outer cutoff specifically of particles as well as walls are used to calculate cohesive forces and equation is given below:

$$F = 2\phi R \left(\left(\frac{h}{h+R} \right) + \frac{1}{\left(1 + \frac{h}{r}\right)^2} \right)$$

$$F_{innercutoff} = 2\pi\phi R \left(\left(\frac{h}{h+R} \right) + \frac{1}{\left(1 + \frac{h}{r_{innercutoff}}\right)^2} \right)$$

While r denotes separation distance, $r_{innercutoff}$ denotes inner cutoff cohesive value in particles, R indicates equivalent Radius, ϕ denotes surface energy and h indicates the impurity. Surface energy denoted by ϕ is:

$$\phi = \frac{A}{24\pi D_0^2}$$

While D_0 denotes the cutoff distance and equals to r for the surface energy. Where A indicates Hamaker constant.

3.7. Particle Size Distribution

In this type of analysis sizes of the particle is uniform. Values are considered for spherical particles at numerous spherical diameters with size of 150um and 150-250um, also mentioned in following table.

Table 3.1. Particle Size Distribution

Particle Type	Mean Spherical Diameter (um)
Small particles	<150 um
Large particles	>150 and <250 um

CHAPTER 4 MODELING TECHNIQUE AND POST PROCESSING

4.1. Modeling Technique:

This process involves multiphase flow with one continuous phase named as primary and other is dispersed within continuous named as secondary and here the diameter is assigned to every secondary phase. Two methods named as Euler-Euler and Eulerian-Lagrangian, are further being classified. Methods employed in multiphase model are described in figure 7. This process employs Discrete Particle method. Mostly researchers use this technique from invention of Laser Metal deposition process to till date. Modeling is performed to forecast outcomes without performing physical phenomenon. This research employs MFix Software which is source multiphase flow solver to calculate the computational technique.

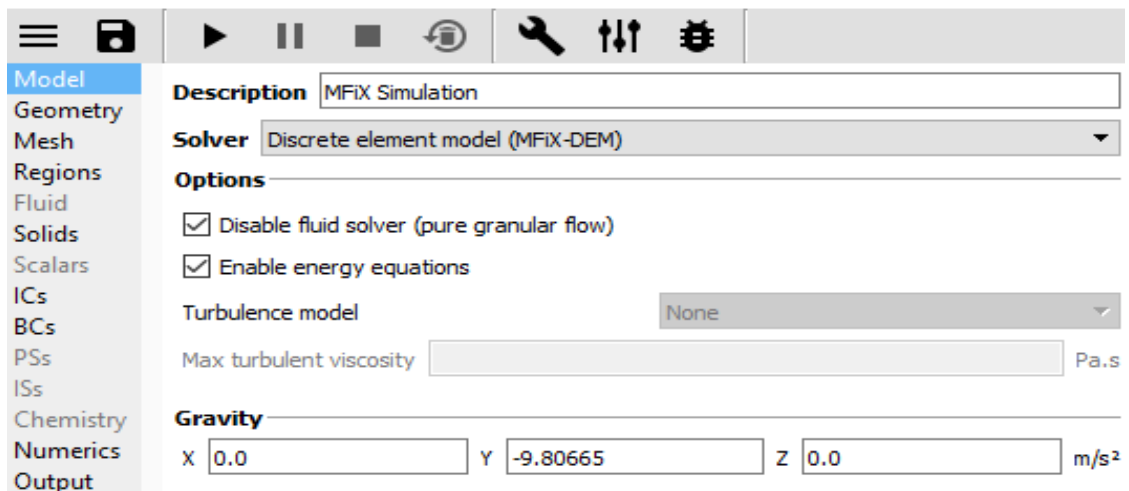


Figure 4.1: Mfix parameters.

i. Introduction:

Many researchers have considered this approach, since the time ‘DLD process’ was invented. Modeling predicts results without physical performance of phenomenon. This study employs MFix Software to compute computational technique

ii. Solver:

Discrete Element Model solver is employed in this process and it employs approach of Lagrange Eulerian (LE).

iii. Governing Equations:

Discrete particles are used to model the solid phase and position, angular velocity and linearity is attained via usage of laws of Newton [14,15,16]. Whereas, equations of fluid phase are similar to MFix EE version. Multiphase flow's vital equations are mentioned below:

$$\varepsilon_f + \sum_{m=1}^m \varepsilon_{sm} = 1$$

Volume fraction of all phases denoted by ε , f and s are fluid as well as solid phase and m refers to mth solid phase, moreover, if solid phases are more than one, their sum make one. While equations for mass and momentum of fluid phase are given below:

$$\frac{\partial}{\partial t}(\varepsilon_f \rho_f) + \nabla \cdot (\varepsilon_f \rho_f \mathbf{v}_f) = 0$$

$$\frac{\partial}{\partial t}(\varepsilon_f \rho_f \mathbf{v}_f) + \nabla \cdot (\varepsilon_f \rho_f \mathbf{v}_f \mathbf{v}_f) = \nabla \cdot \bar{\mathbf{S}}_f + \varepsilon_f \rho_f \mathbf{g} - \sum_{m=1}^M \bar{\mathbf{I}}_f m$$

P refers to density, velocity is denoted by v, \mathbf{S}_f refers to fluid-phase stress tensor, \mathbf{I}_{fm} refers to interphase momentum transfer and gravitational acceleration is denoted by g. Fluid phase is modeled by employing ideal fluid law as compressible fluid:

$$\rho_f = \frac{P_f M_w}{RT_f}$$

Fluid pressure is denoted by P_f , R represents universal gas constant, T_f is temperature of fluid and M_w molecular weight of fluid. But, MFix allow operator to model fluid of phase through stipulation of constant value for fluid density. N_{pm} represents mth solid phase with D_{pm} as diameter of particles and ρ_{sm} as density [17].

Particles total number $N_p = \sum_{m=1}^M N_{pm}$, here M represents solid phases number. Lagrangian frame of reference is used to represent particles at time t

$$\{X^{(i)}(t), V^{(i)}(t), \omega^{(i)}(t), D^{(i)}, \rho^{(i)}, i = 1, \dots, N\},$$

$\rho^{(i)}$ represents density, $D^{(i)}$ denotes to diameter, $V^{(i)}$ is linear velocity, $\omega^{(i)}$ refers to angular velocity and $X^{(i)}$ refers to ith particle's position and ρ_{sm} denotes to density.

Particle belonging to m^{th} solid phase has diameter D_{pm} and density as ρ_{sm} . Mass of particle is product of volume and density.

$$m^{(i)} = \rho^{(i)} \frac{\pi D^{(i)3}}{6}$$

Further, moment of inertia mentioned below:

$$I^{(i)} = \frac{m^{(i)} D^{(i)2}}{10}$$

Linear as well as angular velocities are attained by using the Newtons laws and are given below:

$$\frac{dX^{(i)}(t)}{dt} = V^{(i)}(t)$$

$$m^{(i)} \frac{dV^{(i)}}{dt} = F_T(i) = m^{(i)}g + F_d^{(i)}(t) + F_c^{(i)}(t)$$

$$I^{(i)} \frac{d\omega^{(i)}(t)}{dt} = T^{(i)}$$

X represents particles position at t, $\omega^{(i)}$ refers to angular velocity, V refers to linear velocity and F_d represents drag force which results when particles come in contact with each other.

iv. Data:

Notation	Physical Properties	Unit	316-L-Stainless Steel
----------	---------------------	------	-----------------------

Ts	Solid Temperature	[K]	1630
ρ	Density	[kg/m ³]	8000
Cp(solid)	Specific Heat of solid	[J/kg.K]	500
Hf	Heat of Fusion	[j/g]	260
ϵ	Emissivity		0.2

Factors showing variation in this whole process are termed as Effective variables like laser power and mass flow rate power.

Table 4.1: Factors showing variation in this whole process

v. Upper and Lower Limit of Data:

Numeric variables used in data are required to fill both limits upper as well lower, because it will be defining its limits with variations range.

vi. Material

Computation is performed by using different sizes of Stainless Steel 316L. particles are considered small if they are less than 150um while these are considered large with size from 150-250um. Physical properties given below are of 316L stainless steel which is used in this study.

vii. Shielding Gas:

Argon (Ag) is employed as shielding gas in this process to control depositing particles flow and also to protect the optics.

viii. Model Setup:

Discrete Element Method is the solver used in analysis of this study and drag model named Gidsaspow Polydisperse is employed for analysis of this study.

Numerous variable Process parameters are stated in table 4.2.

Table 4.2. Numerous variable Process parameters

Parameter	Value
-----------	-------

m	Powder flow Rate (g/s)	0.12, 0.18,0.24,0.30
u	Laser Scan Velocity (mm/s)	4
P	Laser Power (W)	800,1000
d	Standoff Distance (mm)	7.5
ρ	Powder Density (g/mm ³)	0.008

ix. Simulation Parameters

Table 4.3: Simulation Parameters

$r_{p_{innercutoff}}$	Minimum Inner Cutoff Particle Radius	40nm
$r_{p_{outercutoff}}$	Maximum Outer Cutoff Particle Radius	500nm
	Surface Asperity Size (h)	5nm
	Wall inner Cutoff Value ($r_{w_{innercutoff}}$)	1 μ m
	Wall outer Cutoff Value ($r_{w_{outercutoff}}$)	5 μ m
	Particle to Particle Spring Constant	10 ⁸ N/m
	Particle to Wall Spring Constant	10 ⁹ N/m

x. Geometry and Meshing:

Geometry is described by usage of geometry pane. It involves whether geometry used and it can be 2D and 3 Dimensional. Further, geometry section offers different tools to add the objects of geometry from STL as well as from any type of primitive elements. Geometry operations are performed by employing Visualization Toolkit Library (VTK).

This study used 3 dimensional geometry. This study made rectangular box of dimensions **50x50x10** mm through this geometry. This 3 dimensional geometry was selected due to few specifications given below:

- Heat transfer was significant at higher power levels
- Flow of the particle was more obvious, when they were falling from the nozzle

. CutCell Mesher was used to perform meshing on MFix. Rectangular box at origin point was given length with corner position. Accordingly, sides of box stretched as per dimensions given in table below. Geometry was selected with the fact that laser beam in the DLD has a spot radius of 1.5mm.

Table 4.4: x-y-z Length

x-length [mm]	y-length[mm]	z-length[mm]
50	50	10

Particles were dropped from the nozzle constantly on rectangular box to fill the space while considering box and the nozzle stationary. Background mesh tab was employed to specify mesh employed by Eulerian solver. Uniform mesh was specified by entering the numbers of cells in the x,y and z directions with the cells in x, y and z direction are of 50,100 and 50 respectively.



Figure4.2: Meshing of Nozzle and Geometry

xi. Laser

Effect of laser is introduced by using constant heat flux. The process was repeated for different laser powers i.e. for 800 and 1000 W. The heat transfer produced by the laser source was calculated via Equation

$$Q = hA\Delta T$$

Where Q is the effect of heat measured in [W], h is the heat transfer coefficient measured in [$\text{W}/\text{m}^2\cdot\text{K}$], A is the area in [m^2] also ΔT is the change in temperature measured in [K].

xii. Mass Flow Rate:

The simulation is done for different values of mass flow rates of powder i.e. 0.12, 0.18, 0.24 and 0.30. And different parameters are observed using these results.

xiii. Setting Solid Phase Initial Values:

Initial Values for solid field variables must be specified for the entire computational domain. The model being solved decree which variables require initial value.

xiv. Volume Fraction:

Initially, the solid phase volume fraction has default value of zero. But in this process, we have assigned the initial value of volume fraction as 0.2. Such that, the sum of all the solid phases volume fractions are used to automatically calculate the volume fraction of fluid phases.



Figure 4.2: Volume fraction of solid particles

xv. Temperature:

The solid phase temperature has a default temperature of 293.15K. It is necessary when solving energy equation.

xvi. Solid Phase Material Properties:

Few material properties are necessary for a specific solid model.

xvii. Diameter:

It is the initial diameter of the particles and will remain constant for reactive as well as non-reactive flows with a variable density. For each case density will remain constant.

xviii. Density:

The particle density is taken as 8000kg/m^3 .

xix. Velocity:

Velocity of 4mm/s is allowed to move particles from nozzle.

xx. Thermal Conductivity:

In this process thermal conductivity is taken as 20(W/mK).

xxi. DEM Settings:

Using DEM tab specific DEM settings are accessed.

xxii. Particle Generation:

Enable automatic particle generation. Using initial condition regions initialize particle location and velocity.

xxiii. Integration Method:

While integrating particle trajectories, the Euler DEM time stepping scheme is used.

xxiv. Collision Model:

Linear Spring dashpot, a soft spring collision model is used in this process.

xxv. Coupling Method:

A fully coupled level of coupling is introduced between the gas and the solid phase

xxvi. Interpolation

A field to particle and particle to field is the interpolation technique that is used for direction of interpolation between field and particle data.

xxvii. Interpolation Scheme

Square DPVM (Divided particle Method Scheme) interpolation scheme is used in this process that requires an interpolation width.

xxviii. Friction Coefficient

Friction Coefficient for both particle-particle and particle-wall are set as 0.4 each. This is required for both LSD and Hertzian Collision Models.

xxix. Normal Spring Constant

Both particle-particle and particle-wall normal spring constants are mentioned as 10^8 and 10^9 (N/m) respectively.

xxx. Restitution Coefficient (Normal)

The value of restitution coefficient is taken as small as we can so that the particles will no bounce back once it falls from nozzle exit. Its value is taken as 0.01. for both particle-particle and particle wall.

xxxi. Fit particles to region (DEM solids only)

This selection is used with the automatic particle generator to expand the initial particle mesh to extent the region.

xxxii. Radiation Temperature

The radiation temperature has a default value of 293.15K, and this is applied when the particles are just existing the nozzle and are entering into the rectangular box.

4.2. Post Processing:

Equivalent spherical particles are moving down due to gravity at the initial speed of 4mm/s into the box as shown in figure. It has been observed that the temperature distribution over the entire region start changing with respect to time is shown in figure 25,26, 27 and 28 at various time intervals. As the particles start entering into the rectangular box from stationary source of particles, the temperature of the box start changing gradually decreases in such a manner that as particles strike the bottom of the box it start cooling as the box is assumed to be placed in atmosphere so radiation temperature boundary condition is applied at that place. At 0.05s particles are just entering into the rectangular box and figure shows that at that interval hot particles temperature start changing. As the particles start touching the bottom of the box, it starts cooling and the figure shown at interval 0.34s indicates the effect of cooling on the deposited layer.

]As the particles start touching the bottom of the box, it starts cooling and the figure shown at interval 0.34s indicates the effect of cooling on the deposited layer.

Also in case of 1000W the effect of temperature on the surface with respect to time is as follows.

When particles enter into the rectangular box, its temperature starts changing and equivalent spherical particles solidifies with the change in temperature as shown in figure. In the next figures, it is illustrated that particles after making first layer, another layer of particles are still dropping over the first one to make another layer over first one such that the layer below the second one is continuously cooling and the later one is at highest temperature than the first and it greatly influence the height of the layer build. The overall sequence of the part build with respect to time is as follows. The red spot in figure 30, indicates the laser source where the temperature is changing. The particles start spreading in the geometry until all the particles present in the nozzle dropped into the box to achieve the layer deposition of the particles. At 0.13s , It has been observed that the deposited layer is much thicker and denser than the figure before. The figure below will show the result when all the particles are deposited layer by layer and the layer touching the bottom of the box will cool first and the layer after it will cool after depositing that layer and the effect of it is shown below. It has been observed that the layer height obtained at different mass flow rates and powers by altering the values of mass flow rates and laser powers, the following are the graphs obtained for equivalent spherical particles are as follows:

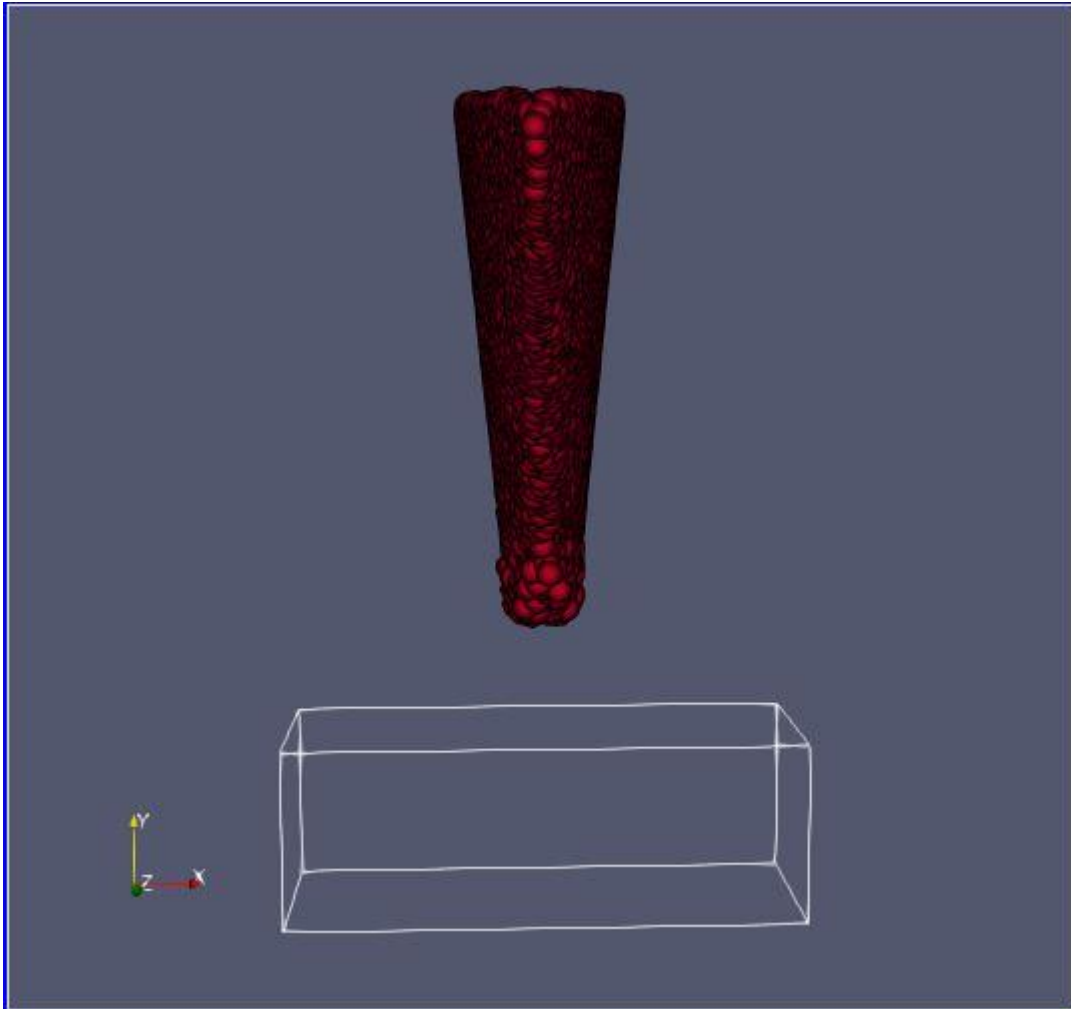


Figure 4.3: Particles Motion through nozzle into bed

4.3. Temperature Distribution:

The temperature distribution over the entire region is shown below at various time intervals. As the particles start entering into the rectangular box from stationary source of particles, the temperature of the box start changing gradually decreases in such a manner that as particles strike the bottom of the box it start cooling as the box is assumed to be placed in atmosphere so radiation temperature boundary condition is applied at that place. At 0.05s particles are just entering into the rectangular box and figure shows that at that interval hot particles temperature start changing.

As the particles start touching the bottom of the box, it starts cooling and the figure shown at interval 0.34s indicates the effect of cooling on the deposited layer.

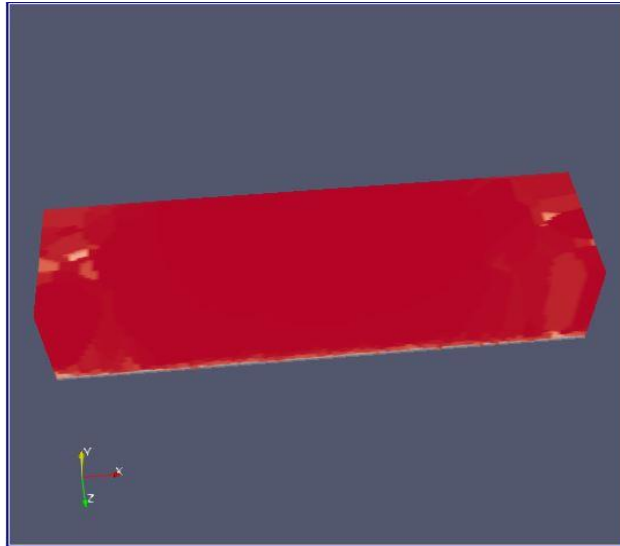


Figure 4.4: Temperature Distribution at 0.05s

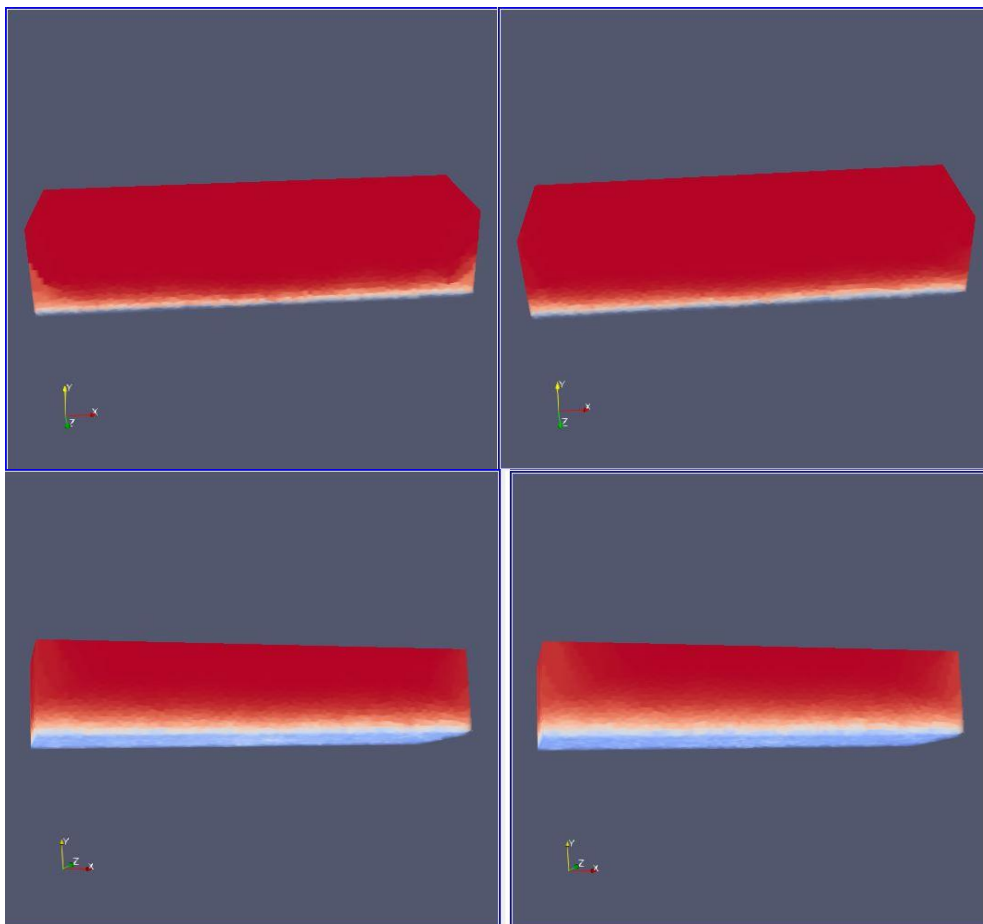


Figure 4.5.: Temperature Distribution at 0.1s, 0.2, 0.3 and 0.4s

The effect of heating can also be illustrated using the following diagram at 0.05s.

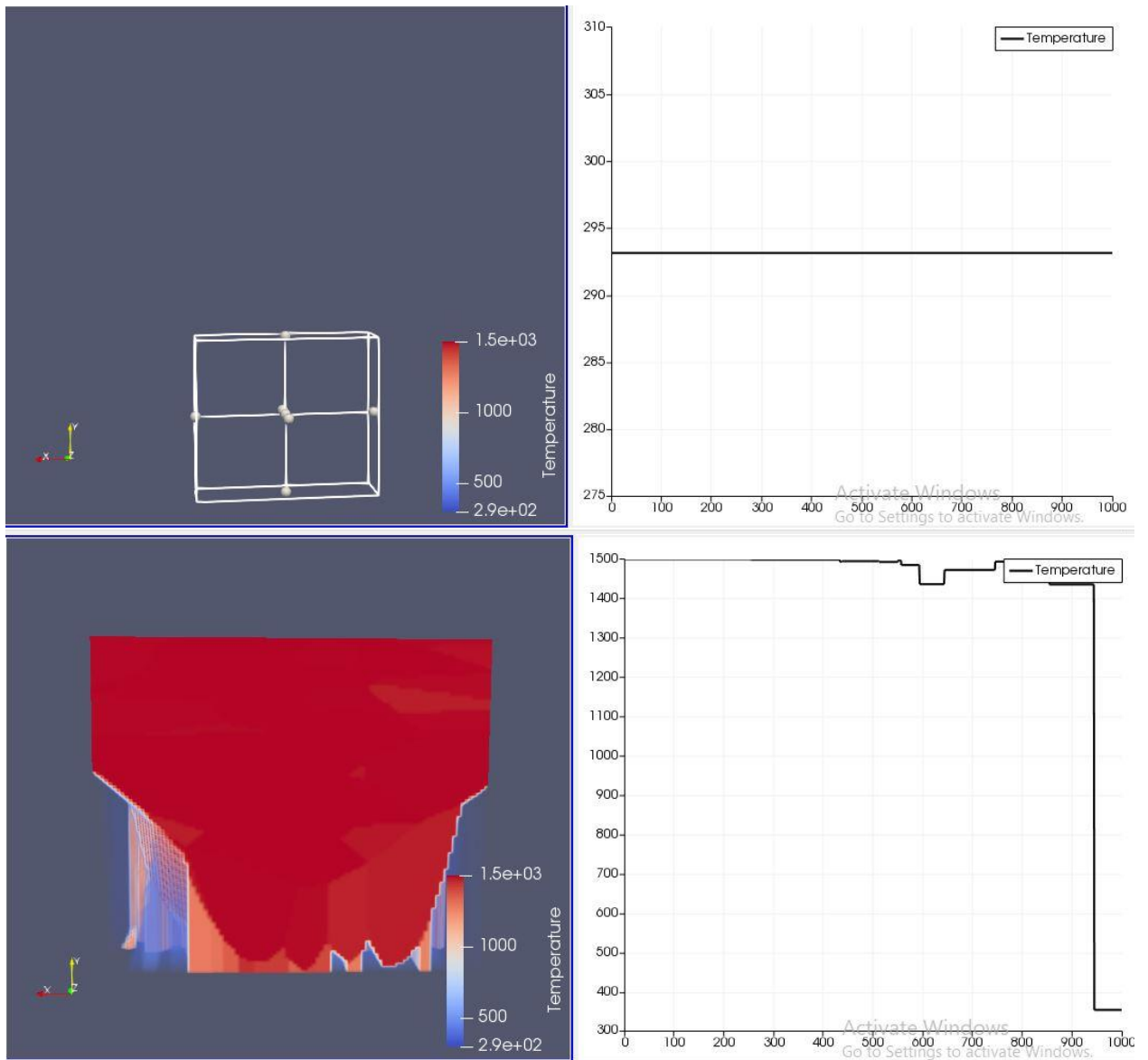


Figure 4.6: Temperature distribution at 00, 0.1,0.2s

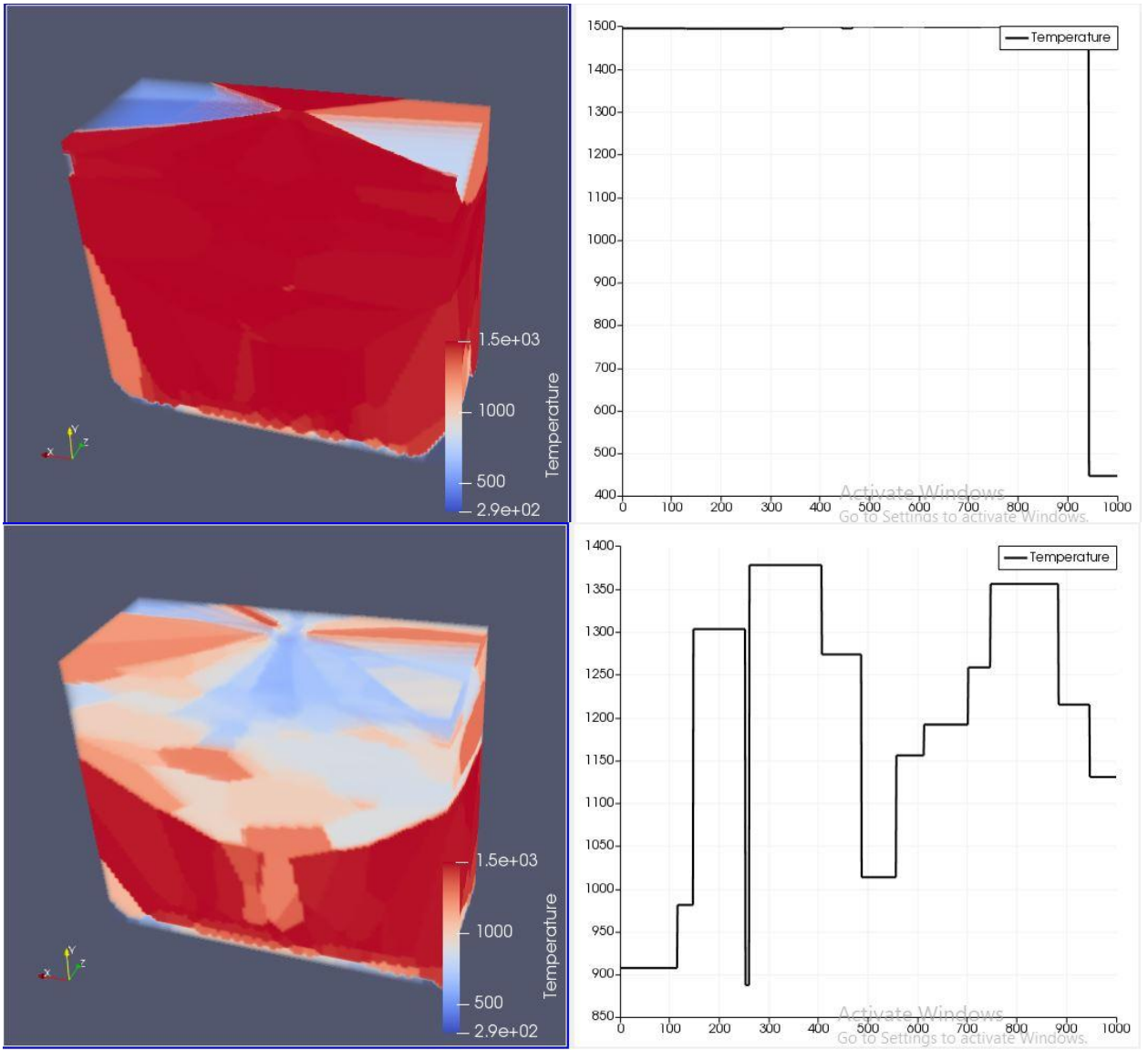
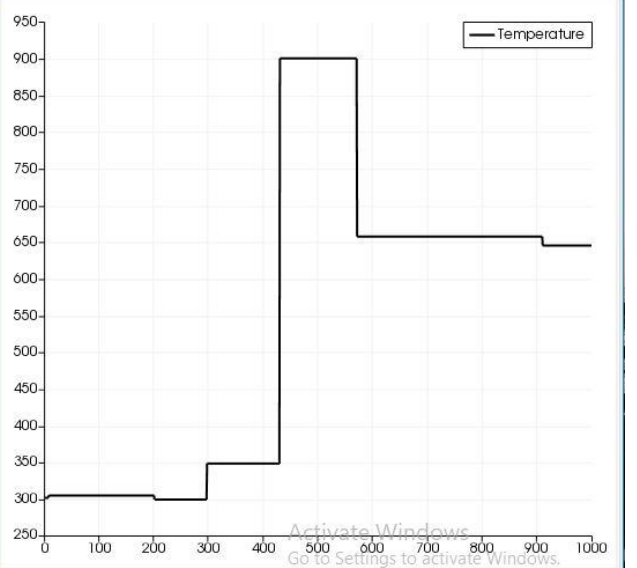
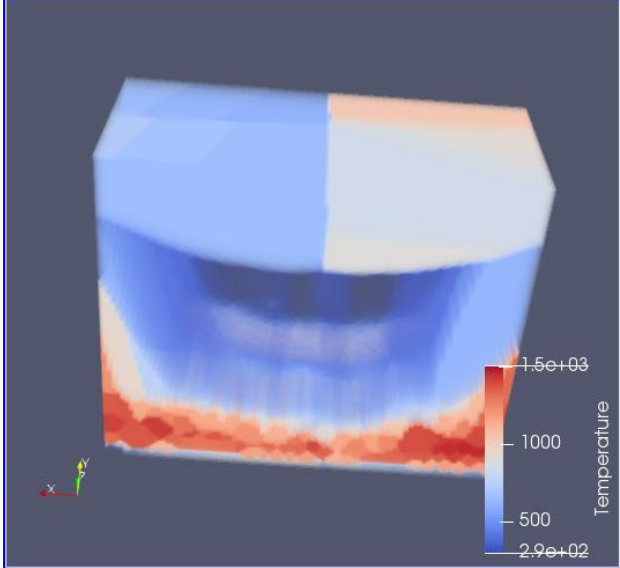
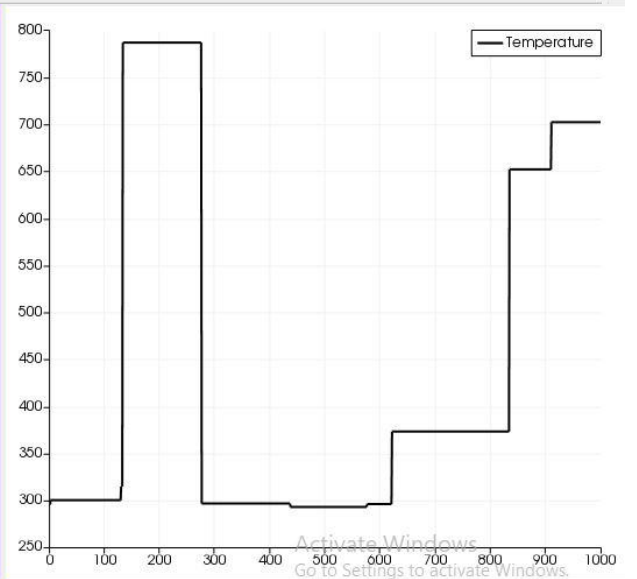
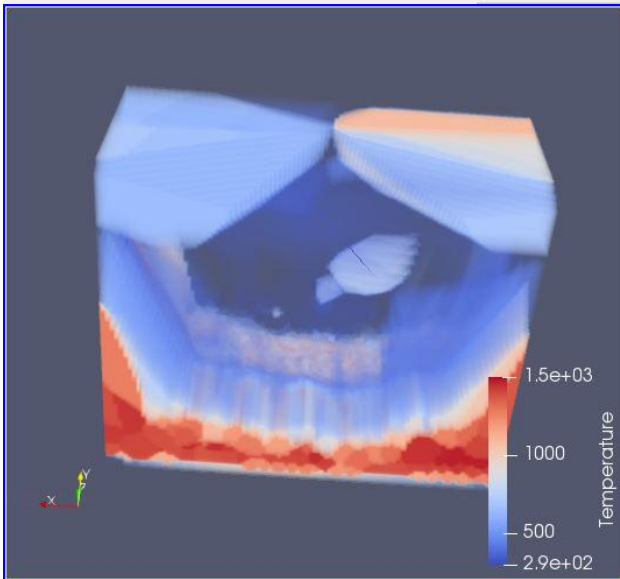
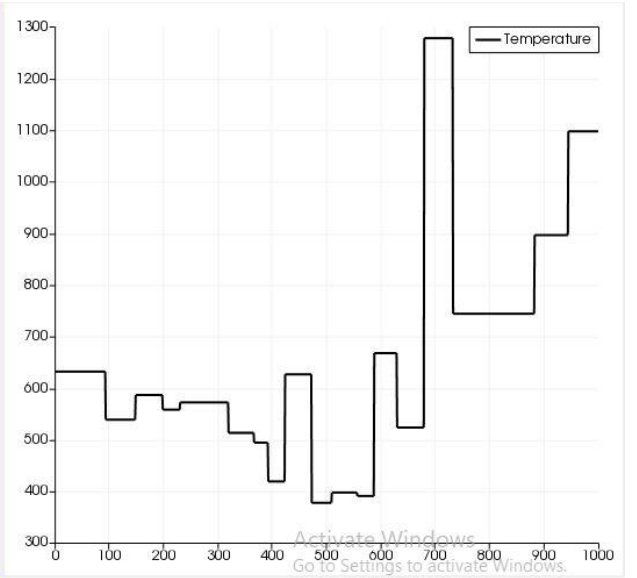
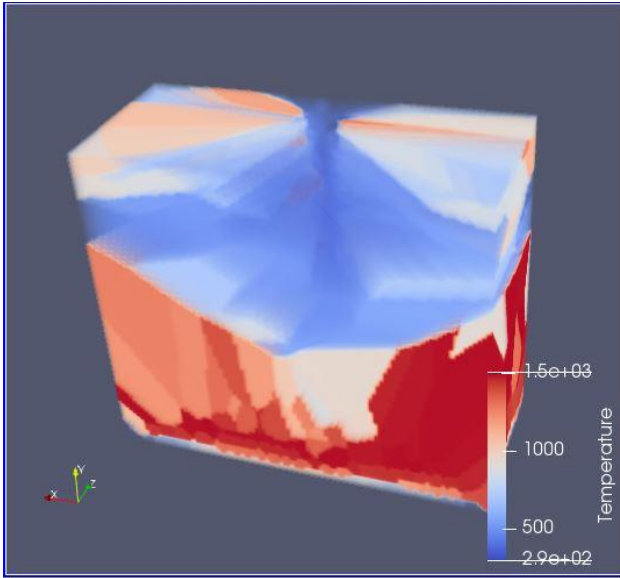
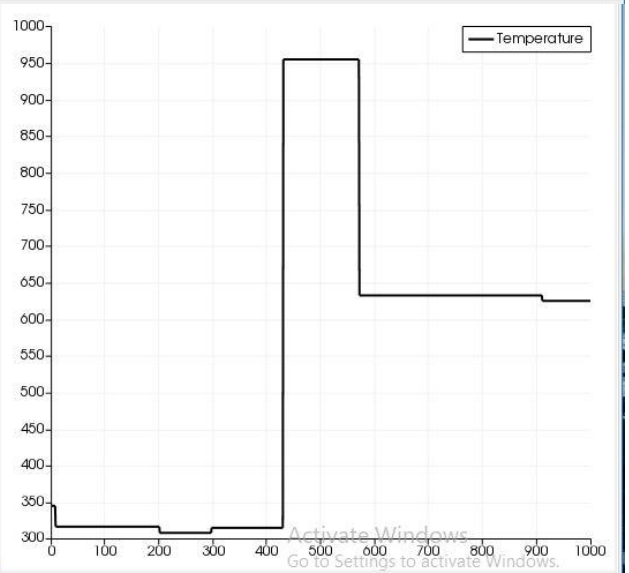
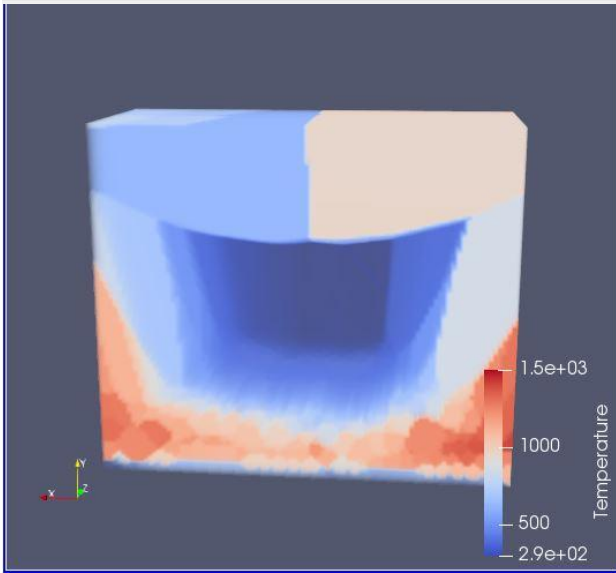
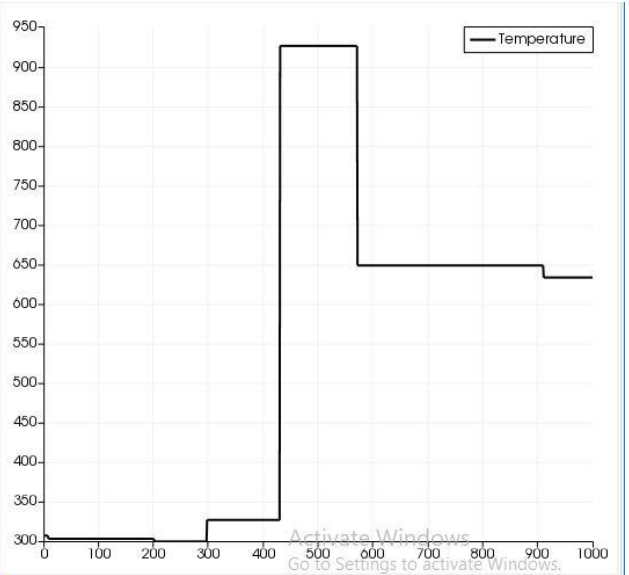
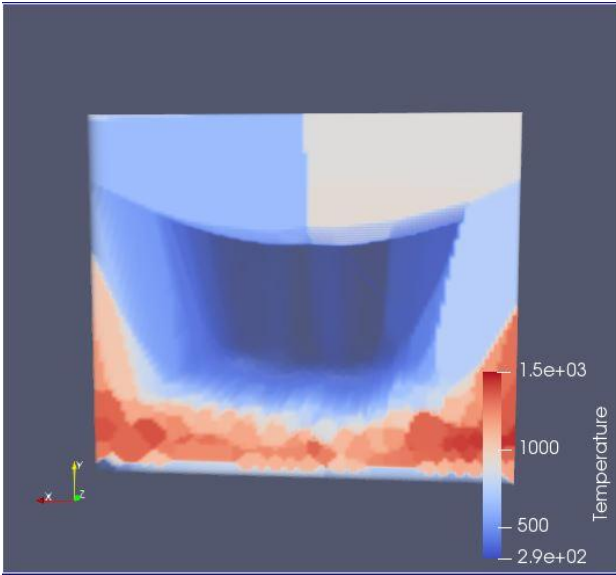


Figure 4.7: Temperature distribution at 0.28,0.333,0.4s





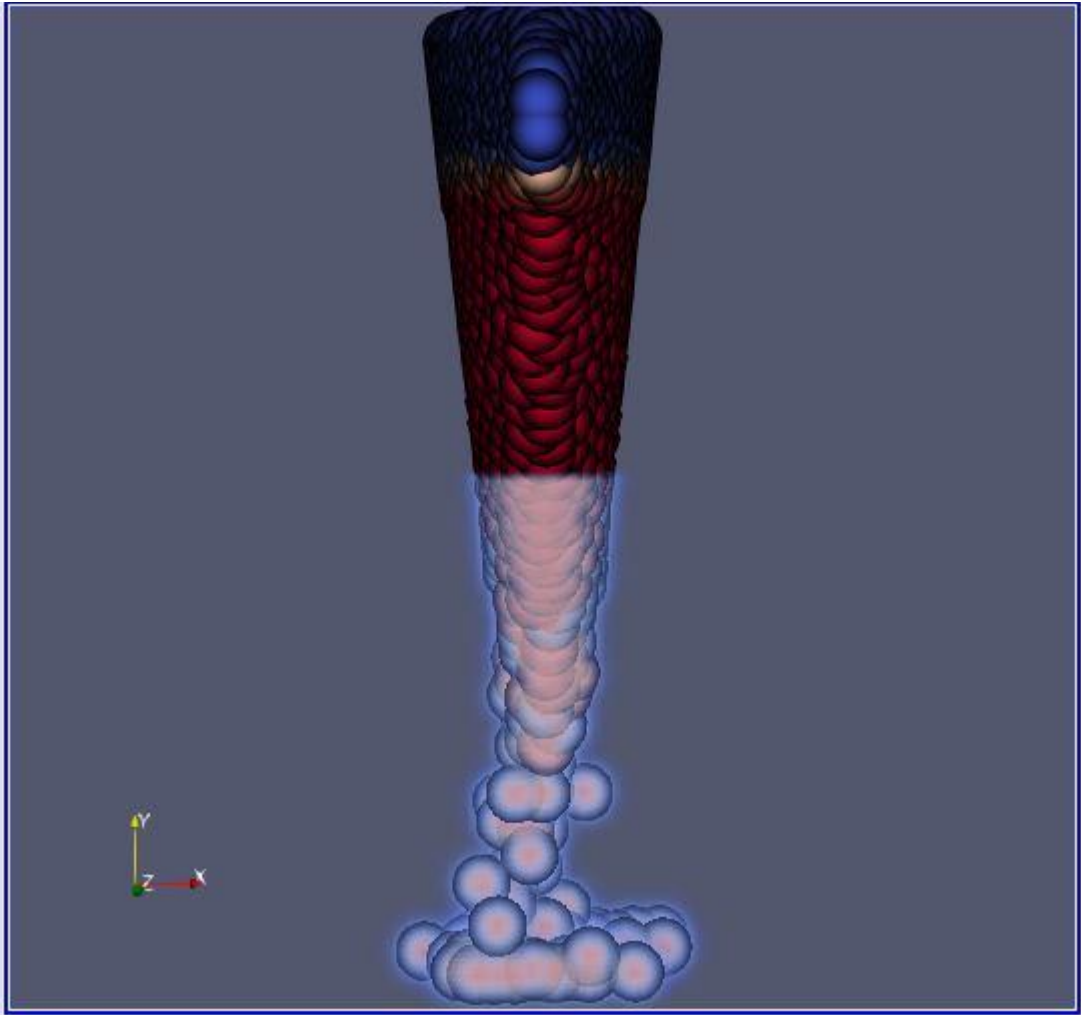


Figure 4.8: Particle Drop through nozzle

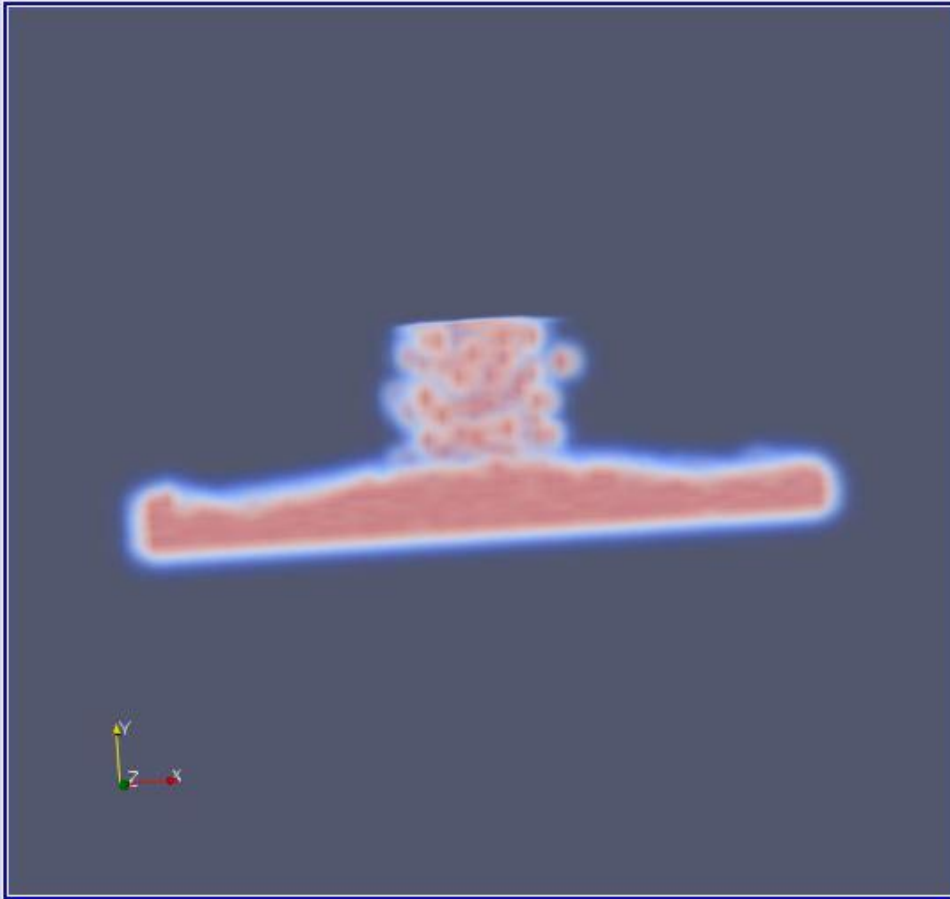


Figure 4.9: Layer Formation

The red spot indicates the exit of the nozzle where the temperature is changing. The particles start spreading in the geometry until all the particles present in the nozzle dropped into the box to achieve the layer deposition of the particles.

At 0.13s , It has been observed that the deposited layer is much thicker and denser than the figure before.

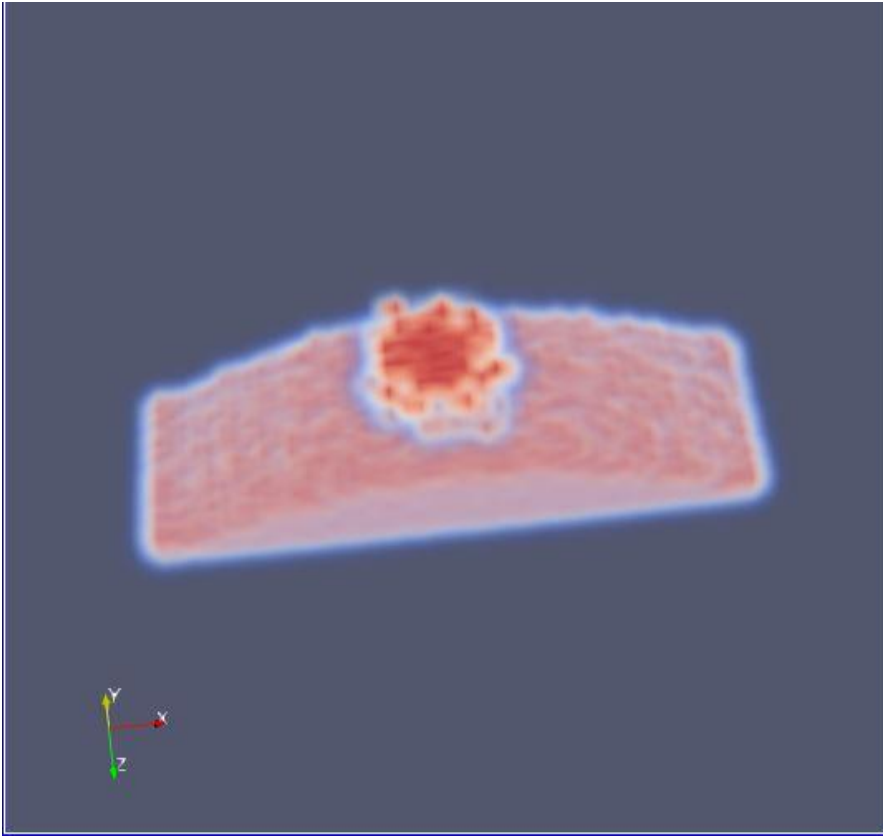


Figure 4.10: Layer Formation

The figure below will show the result when all the particles are deposited layer by layer and the layer touching the bottom of the box will cool first and the layer after it will cool after depositing that layer and the effect of it is shown below.

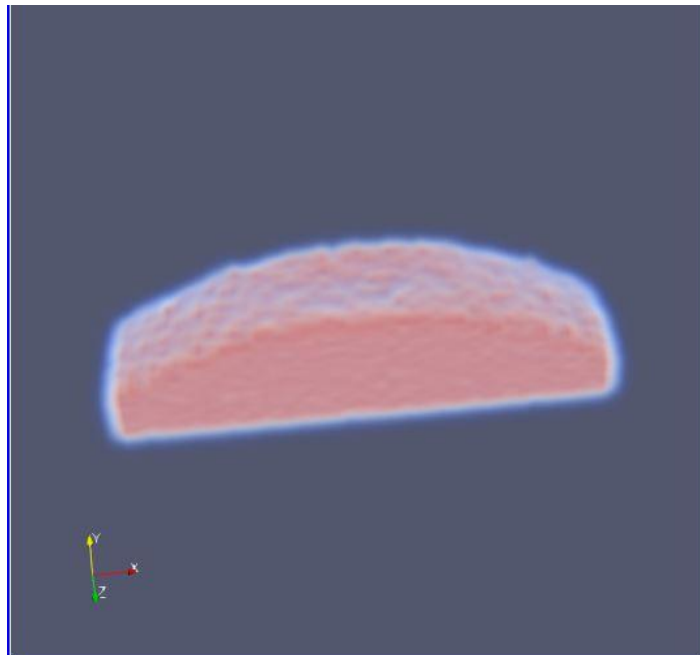


Figure4.11: Layer Formation

It has been observed that the layer height obtained at different mass flow rates and power are as follows:

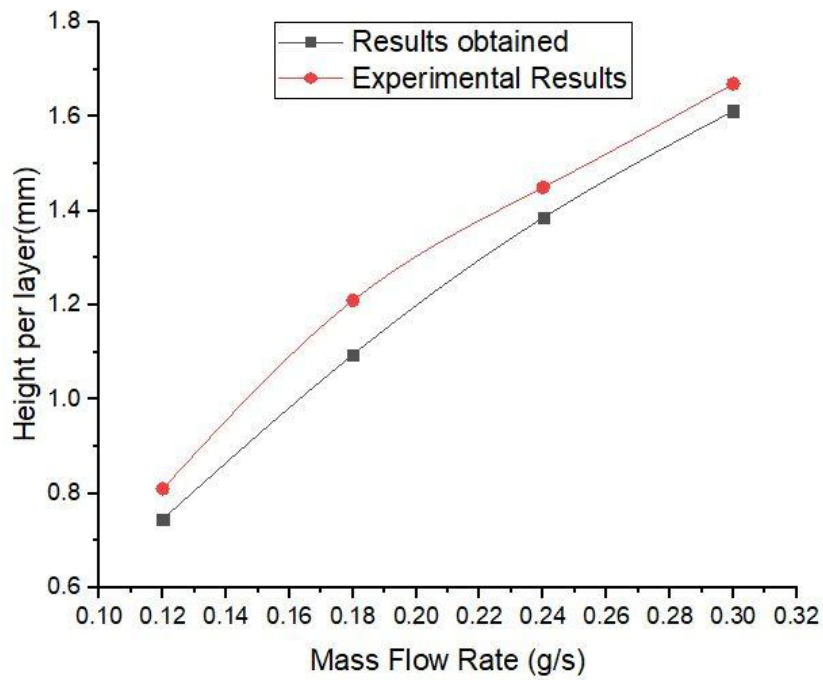


Figure 4.12: Mass flow rate vs layer build height of small particles at 800W

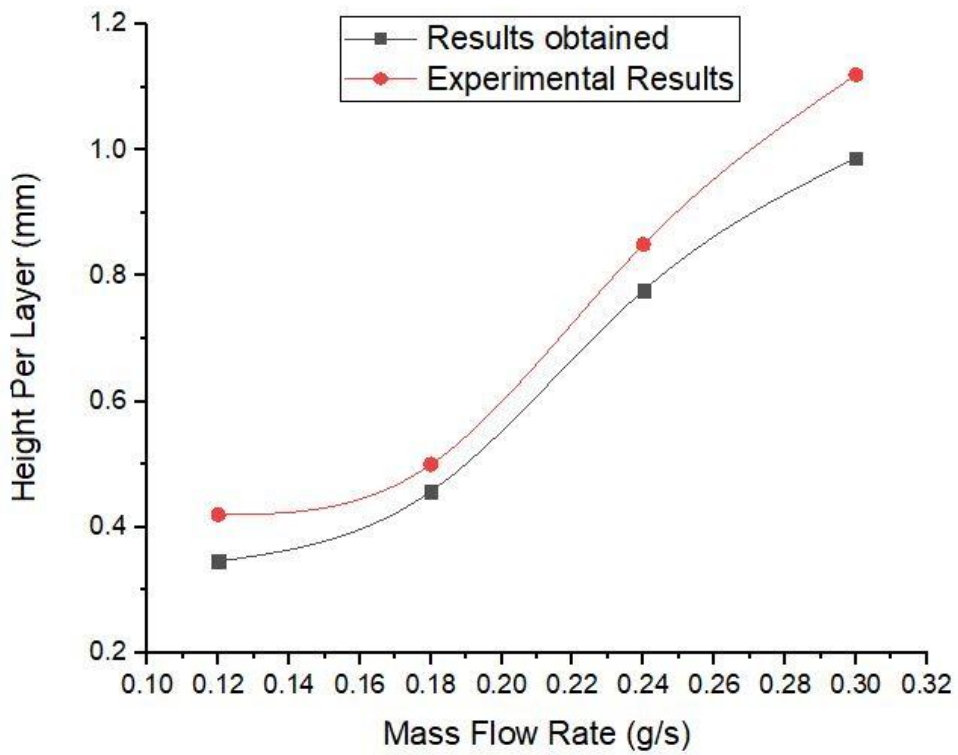


Figure 4.13: Mass flow rate vs layer build height of large particles at 800W

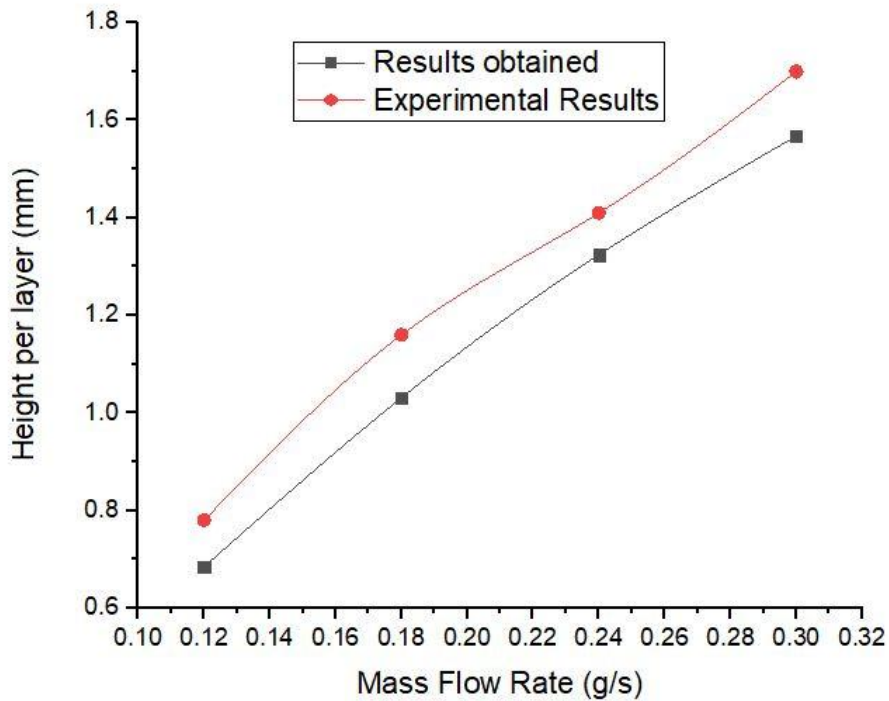


Figure 4.14: Mass flow rate vs layer build height of small particles at 1000W

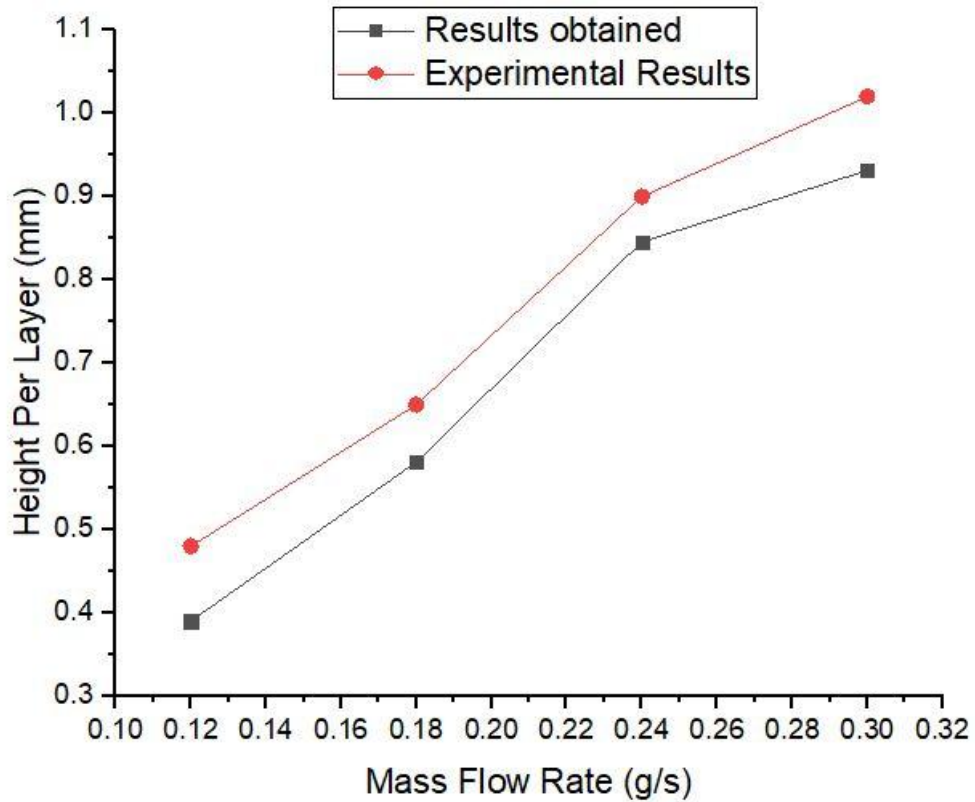


Figure4.15: Mass flow rate vs layer build height of large particles at 1000W

It has been observed that the experimental results are in good agreement with the experimental one when the particles are small. As the laser power increases from 800W to 1000W, layer height will also increase to some extent showing optimization in the results, but after that increase in laser power will cause reduction in laser height. As the laser power increases temperature increases and high temperature causes the liquid viscosity to decrease, accordingly

CHAPTER 5 RESULTS AND DISCUSSIONS:

Impact of mass flow rate as well as power of laser on solid region of melt pool boundary was determined by conducting discrete element method. With small particles results were in accordance with experimental results. Layer height was increased when laser power was increased from 800W to 1000W which showed optimization in results. But, further increase in laser power would decrease laser height. With increase in laser power, temperature also increases which leads to decrease in liquid viscosity and hence material may be extended . Moreover, on change of layer deposition, particles morphology was also changed. With increase in particles size, distribution of temperature is changed and as a result more energy is absorbed by large particles effecting the melt pool because more energy is needed to melt the big particles which decreases deposited height. Particles when changed from Small particles to Large particles, layer height is decreased. Hence, it is concluded that morphology of particles is important as it effects the process. Particle when changes its particle size may effect particle concentration, energy attenuation and temperature distribution.

REFERENCES

- [1]. Graf, B.; Ammer, S.; Gumenyuk, A.; Rethmeier, M. Design of experiments for DLD in maintenance, repair and overhaul applications. *Procedia CIRP* **2013**, 11, 245–248. [CrossRef]
- [2]. Song, J.; Deng, Q.; Chen, C.; Hu, D.; Li, Y. Rebuilding of metal components with laser cladding forming. *Appl. Surf. Sci.* **2006**, 252, 7934–7940. [CrossRef]
- [3]. Yao, Y.; Huang, Y.; Chen, B.; Tan, C.; Su, Y.; Feng, J. Influence of processing parameters and heat treatment on the mechanical properties of 18Ni300 manufactured by laser based directed energy deposition. *Opt. Laser Technol.* **2018**, 105, 171–179. [CrossRef]
- [4]. Caiazzo, F.; Alfieri, V. Laser-aided Directed Energy Deposition of steel powder over flat surfaces and edges. *Materials* **2018**, 11, 435. [CrossRef] [PubMed]
- [5]. Koike, R.; Misawa, T.; Aoyama, T.; Kondo, M. Controlling metal structure with remelting process in direct energy deposition of Inconel 625. *CIRP Ann.* **2018**, 67, 237–240. [CrossRef]
- [6]. Koike, R.; Matsumoto, T.; Kakinuma, Y.; Aoyama, T.; Oda, Y.; Kondo, T.K.e.M. A basic study on metal foam fabrication with titanium hydride in direct energy deposition. *Procedia Manuf.* **2018**, 18, 68–73. [CrossRef]
- [7]. Lee H, Lim CHJ, Low MJ, Tham N, Murukeshan VM, Kim YJ (2017) Lasers in additive manufacturing: a review. *Int J Precis Eng Manuf-Green Technol* 4:307–322. <https://doi.org/10.1007/s40684-017-0037-7>
- [8]. Taminger K, Hafley R (2003) Electron beam freeform fabrication: a rapid metal deposition process. *Proceedings of the 3rd Annual Automotive Composites Conference*
- [9]. Stecker S, Lachenberg K, Wang H, Salo R (2006) Advanced electron beam free form fabrication methods & technology. *Amer Weld Soc Conf* 17:35–46
- [10]. Kakinuma Y, Mori M, Oda Y, Mori T, Kashihara M, Hansel A, Fujishima M (2016) Influence of metal powder characteristics on product quality with directed energy deposition of Inconel 625. *CIRP Ann* 65:209–212. <https://doi.org/10.1016/j.cirp.2016.04.058>

- [11]. Herali'c A, Christiansson AK, Lennartson B (2012) Height control of laser metal-wire deposition based on iterative learning control and 3D scanning. *Opt Lasers Eng* 50:1230–1241. <https://doi.org/10.1016/j.optlaseng.2012.03.016>
- [12]. Syed WUH, Pinkerton AJ, Li L (2005) A comparative study of wire feeding and powder feeding in direct diode laser deposition for rapid prototyping. *Appl Surf Sci* 247:268–276.
<https://doi.org/10.1016/j.apsusc.2005.01.138>
- [13]. Syed WUH, Pinkerton AJ, Li L (2006) Combining wire and coaxial powder feeding in laser direct metal deposition for rapid prototyping. *Appl Surf Sci* 252:4803–4808.
<https://doi.org/10.1016/j.apsusc.2005.08.118>
- [14]. Costa L, Vilar R (2009) Laser powder deposition. *Rapid Prototyp J* 15:264–279.
<https://doi.org/10.1108/13552540910979785>
- [15]. Collins PC, Banerjee R, Banerjee S, Fraser HL (2003) Laser deposition of compositionally graded titanium-vanadium and titanium-molybdenum alloys. *Mater Sci Eng A* 352:118–128.
[https://doi.org/10.1016/s0921-5093\(02\)00909-7](https://doi.org/10.1016/s0921-5093(02)00909-7)
- [16]. Wu D, Liang X, Li Q, Jiang L (2010) Laser rapid manufacturing of stainless steel 316l/Inconel718 functionally graded materials: microstructure evolution and mechanical properties. *Int J Opt* 2010:1–5. <https://doi.org/10.1155/2010/802385>
- [17]. Reichardt A, Dillon RP, Borgonia JP, Shapiro AA, McEnerney BW, Momose T, Hosemann P (2016) Development and characterization of Ti-6Al-4V to 304l stainless steel gradient components fabricated with laser deposition additive manufacturing *Mater Des* 104:404–413. <https://doi.org/10.1016/j.matdes.2016.05.016>
- [18]. Korinko P, Adams T, Malene S, Gill D, Smugeresky J (2011) Laser engineered net shaping® for repair and hydrogen compatibility. *Weld J* 90:171–181
- [19]. Fang J, Dong S, Li S, Wang Y, Xu B, Li J, Liu B, Jiang Y (2019) Direct laser deposition as repair technology for a low transformation temperature alloy: microstructure, residual stress, and properties. *Mater Sci Eng A* 748:119–127.
<https://doi.org/10.1016/j.msea.2019.01.072>
- [20]. Zhang X, Pan T, Li W, Liou F (2019) Experimental characterization of a direct metal deposited cobalt-based alloy on tool steel for component repair. *JOM* 71:946–955. <https://doi.org/10.1007/s11837-018-3221-5>

- [21]. Hy Zhao, Ht Zhang, Xu Ch, Xq Yang (2009) Temperature and stress fields of multi-track laser cladding. *Trans Nonferrous Metals Soc China* 19:s495–s501. [https://doi.org/10.1016/s1003-6326\(10\)60096-9](https://doi.org/10.1016/s1003-6326(10)60096-9)
- [22]. Scheitler C, Hugger F, Hofmann K, Hentschel O, Baetzler T, Roth S, Schmidt M (2016) Experimental investigation of direct diamond laser cladding in combination with high speed camera based process monitoring. *J Laser Appl* 28:022304. <https://doi.org/10.2351/1.4944004>
- [23]. Griffith M, Keicher D, Atwood C, Romero J, Smugeresky J, Harwell L, Greene D (1996) Free form fabrication of metallic components using laser engineered net shaping (LENS™). *Proceedings of the Solid Freeform Fabrication Symposium*, pp 125–131
- [24] T.B. Anderson, R. Jackson, 1967, A fluid mechanical description of fluidized beds.
- [25] M. Ishii, 1975, *Thermo-Fluid Dynamic Theory of Two-Phase Flow*, Eyrolles, Paris . [26] D. Gidaspow, 1994, *Multiphase Flow and Fluidization: Continuum and Kinetic Theory*
- [27] C.K.K. Lun, 1984, Kinetic theories for granular flow inelastic particles in Couette flow and slightly inelastic particles in a general flow field *Journal of Fluid Mechanics* 140
- [28] D. Gidaspow, 1983, London Fluidization in two-dimensional beds with a jet, *Industrial and Engineering Chemistry Fundamentals* 22 (2) (1983) 193–201.
- [29] Y.P. Tsuo, 1990, *Computation of flow patterns in circulating fluidized beds*, Paris
- [30] M.A. van der Hoef, 2006, *Multiscale modeling of gas-fluidized beds*, Paris [8] G.V. Middleton, 1984, *Mechanics of Sediment Movement* 2nd ed Society of Economic Paleontologists and Mineralogists, Tulsa OK.
- [31] A. Prosperetti, 2007, *Computational Methods for Multiphase Flow*, 1st ed, Cambridge University Press.

- [32] C.T. Crowe, 2011, *Multiphase Flows with Droplets and Particles*, Boca Raton.
- [33] P. Gondret, 2002, Bouncing motion of spherical particles in fluids, *Phys Fluids* 14 643
- [34] ASTM International Committee F42 on Additive Manufacturing Technologies, *ASTM F2792–10 Standard Terminology for Additive Manufacturing Technologies*, ASTM, West Conshohocken, PA, 2009. [35] N. Guo, M. C. Leu, *Additive Manufacturing: Technology, Applications and Research Needs*, *Front. Mech. Eng.*, 8(3), (2013), 215-243.
- [36] William J. Seufzer, *Additive Manufacturing Modeling and Simulation: A Literature Review for Electron Beam Free Form Fabrication*, NASA/TM–2014-218245, (2014)
- [37] V. P. Carey, *DLD using Alloy 718 Powder*. University West, SE-46186, Trollhättan Sweden: PhD Thesis, Production Technology, 2017.
- [38] “Hybrid Manufacturing Technologies.” <http://www.hybridmanutech.com>. Accessed: 2019-02-07
- [39] Mahamood, R.M., Akinlabi, E.T., Shukla, M. and Pityana, S., 2014. Characterization of laser deposited Ti6Al4V/TiC composite powders on a Ti6Al4V substrate.
- [40] Thayalan, V. and Landers, R.G., 2006. Regulation of powder mass flow rate in gravity-fed powder feeder systems. *Journal of manufacturing processes*, 8(2), pp.121-132.
- [41] Rein, G. and Andrés, A., 2001. Computer simulation of granular material: vibrating feeders. *Powder Handling & Processing*, 13(2), pp.181-185.
- [42] Huang, Y., Khamesee, M.B. and Toyserkani, E., 2016. A comprehensive analytical model for laser powder-fed additive manufacturing. *Additive Manufacturing*, 12, pp.90-99.
- [43] Tang, H.P., Qian, M., Liu, N., Zhang, X.Z., Yang, G.Y. and Wang, J., 2015. Effect of powder reuse times on additive manufacturing of Ti-6Al-4V by selective electron beam melting. *Jom*, 67(3), pp.555-563.

- [44] Le Bourhis, F., Kerbrat, O., Dembinski, L., Hascoet, J.Y. and Mognol, P., 2014. Predictive model for environmental assessment in additive manufacturing process. *Procedia CiRP*, 15, pp.26-31.
- [45] Bhavar, V., Kattire, P., Patil, V., Khot, S., Gujar, K. and Singh, R., 2014, September. A review on powder bed fusion technology of metal additive manufacturing. In 4th International Conference and Exhibition on Additive Manufacturing Technologies-AM-2014, September (pp. 1-2).
- [46] Lagutkin, S., Achelis, L., Sheikhaliev, S., Uhlenwinkel, V. and Srivastava, V., 2004. Atomization process for metal powder. *Materials Science and Engineering: A*, 383(1), pp.1-6.
- [47] Pinkerton, A.J. and Li, L., 2005. Direct additive laser manufacturing using gas- and water-atomised H13 tool steel powders. *The International Journal of Advanced Manufacturing Technology*, 25(5-6), pp.471-479.
- [48] Witzel, J., Kelbassa, I., Gasser, A. and Backes, G., 2010, September. Increasing the deposition rate of Inconel 718 for DLD. In *International Congress on Applications of Lasers & Electro-Optics (Vol. 2010, No. 1, pp. 304-310)*. LIA.
- [49] Aldrich, R., 2000. *Laser fundamentals*.
- [50] Ding, K. and Ye, L., 2006. *Laser shock peening: performance and process simulation*. Woodhead Publishing.
- [51] Mahamood, R.M. and Akinlabi, E.T., 2017. Scanning speed influence on the microstructure and micro hardness properties of titanium alloy produced by DLD process. *Materials today: Proceedings*, 4(4), pp.5206-5214.
- [52] Konert, M. and Vandenberghe, J.E.F., 1997. Comparison of laser grain size analysis with pipette and sieve analysis: a solution for the underestimation of the clay fraction. *Sedimentology*, 44(3), pp.523-535.
- [53] Vigneau, E., Loisel, C., Devaux, M.F. and Cantoni, P., 2000. Number of particles for the determination of size distribution from microscopic images. *Powder Technology*, 107(3), pp.243-250.

- [54] Eshel, G., Levy, G.J., Mingelgrin, U. and Singer, M.J., 2004. Critical evaluation of the use of laser diffraction for particle-size distribution analysis. *Soil Science Society of America Journal*, 68(3), pp.736-743.
- [55] Zhang, Y., Xi, M., Gao, S. and Shi, L., 2003. Characterization of laser direct deposited metallic parts. *Journal of materials processing technology*, 142(2), pp.582-585.
- [56] Huang, Y.L., Liu, J., Ma, N.H. and Li, J.G., 2006. Three-dimensional analytical model on laser-powder interaction during laser cladding. *Journal of Laser Applications*, 18(1), pp.42-46.
- [57] Fu, Y., Loredo, A., Martin, B. and Vannes, A.B., 2002. A theoretical model for laser and powder particles interaction during laser cladding. *Journal of Materials Processing Technology*, 128(1-3), pp.106-112.

CERTIFICATE OF COMPLETENESS

It is hereby certified that the dissertation submitted by *NS Zia ur rehman Sarwar*,
Registration

No.000002005599, Titled: “*Modeling the Effect of Spherical Particles of various
Sizes using Direct Laser Deposition* ” has been checked/reviewed and its contents are
complete in all respects.



Signature of Supervisor
(Dr. Khalid Mahmood)